Environmental Research 159 (2017) 186–201

Contents lists available at ScienceDirect

Environmental Research

journal homepage: www.elsevier.com/locate/envres

Combustion-derived nanoparticles, the neuroenteric system, cervical vagus, hyperphosphorylated alpha synuclein and tau in young Mexico City residents

Lilian Calderón-Garcidueñas[a,b,*], Rafael Reynoso-Robles[c], Beatriz Pérez-Guillé[c], Partha S. Mukherjee[d], Angélica Gónzalez-Maciel[c]

[a] The University of Montana, Missoula, MT 59812, USA
[b] Universidad del Valle de México, Mexico City 14370, Mexico
[c] Instituto Nacional de Pediatría, Mexico City 04530, Mexico
[d] Mathematics Department, Boise State University, Boise, Idaho, USA

ARTICLE INFO

Keywords:
Alzheimer
Alpha synuclein
Combustion-derived nanoparticles
Children
GI barrier
Hyperphosphorylated tau
Neuroenteric system
Mexico City
Parkinson
Vagus

ABSTRACT

Mexico City (MC) young residents are exposed to high levels of fine particulate matter ($PM_{2.5}$), have high frontal concentrations of combustion-derived nanoparticles (CDNPs), accumulation of hyperphosphorylated aggregated α-synuclein (α-Syn) and early Parkinson's disease (PD). Swallowed CDNPs have easy access to epithelium and submucosa, damaging gastrointestinal (GI) barrier integrity and accessing the enteric nervous system (ENS). This study is focused on the ENS, vagus nerves and GI barrier in young MC v clean air controls. Electron microscopy of epithelial, endothelial and neural cells and immunoreactivity of stomach and vagus to phosphorylated α-synuclein Ser129 and Hyperphosphorylated-Tau (Htau) were evaluated and CDNPs measured in ENS. CDNPs were abundant in erythrocytes, unmyelinated submucosal, perivascular and intramuscular nerve fibers, ganglionic neurons and vagus nerves and associated with organelle pathology. αSyn and Htau were present in 25/27 MC gastric,15/26 vagus and 18/27 gastric and 2/26 vagus samples respectively. We strongly suggest CDNPs are penetrating and damaging the GI barrier and reaching preganglionic parasympathetic fibers and the vagus nerve. This work highlights the potential role of CDNPs in the neuroenteric hyperphosphorylated α-Syn and tau pathology as seen in Parkinson and Alzheimer's diseases. Highly oxidative, ubiquitous CDNPs constitute a biologically plausible path into Parkinson's and Alzheimer's pathogenesis.

1. Introduction

Mexico City (MC) children, teens and young adults exhibit the neuropathological hallmarks of Alzheimer and Parkinson's diseases i.e., tau hyperphosphorylation with pre-tangles, amyloid beta42 (Aβ42) diffuse and mature plaques, and misfolded α-synuclein olfactory bulb and brainstem accumulation (Calderón-Garcidueñas et al., 2008, 2010, 2011, 2012, 2013a, 2013b; Villarreal-Calderon et al., 2010). Lewy neurites and/or punctuate α-synuclein deposits in the olfactory bulb, trigeminal thalamic tract, mesencephalic V, reticular and raphe nuclei, the glossopharyngeal-vagus complexes and lung and heart autonomic ganglia are seen in MC v control children as young as 11 years old (Calderón-Garcidueñas et al., 2011, 2013a, 2013b). We have shown upregulation of COX2 in the right vagus and of CD14 in both right and left vagus of teens and young MC adults suggesting the vagus nerve plays a role in the brainstem inflammation and neurodegeneration process (Calderón-Garcidueñas et al., 2008). In highly exposed MC Balb-c mice, dorsal vagal complex (DVC) inflammation is a robust finding strongly associated with DVC imbalance in genes associated with antioxidant defenses, apoptosis, and neurodegeneration (Villarreal-Calderon et al., 2010).

Data in the literature support an association between air pollutants (ozone, fine particulate matter $PM_{2.5}$ and/or lead) and higher risk of Parkinson's disease (Kirrane et al., 2015, Santurtún et al., 2016), while others find limited evidence between exposures to ambient particulate matter (PM_{10}, $PM_{2.5}$) or nitrogen oxides (NO_2), and PD risk (Liu et al., 2016; Chen et al., 2017; Calderón-Garcidueñas and Villarreal-Ríos, 2017). Interestingly, the experimental combination of ultrafine carbon black and rotenone -a pesticide used to induce dopaminergic (DA) damage-, work synergistically to activate NADPH oxidase in microglia, leading to DA neurons oxidative damage (Wang et al., 2017). There is no doubt however of the capacity of nanoparticles (NPs) to produce DA

* Correspondence to: The University of Montana, 287 Skaggs Building, 32 Campus Drive, Missoula, MT 59812, USA.
E-mail address: lilian.calderon-garciduenas@umontana.edu (L. Calderón-Garcidueñas).

http://dx.doi.org/10.1016/j.envres.2017.08.008
Received 5 June 2017; Received in revised form 2 August 2017; Accepted 4 August 2017
Available online 10 August 2017

damage (Hu et al., 2017; Xie et al., 2016; Imam et al., 2015; Levesque et al., 2011a, 2011b, 2013). Of special interest is the work of Levesque and coworkers (Levesque et al., 2011a, 2011b, 2013) showing the effect of diesel NPs upon microglia, neuroinflammation, and DA neurotoxicity. The combination of diesel NPs and lipopolysaccharide (LPS) (2.5 ng/mL) in vitro synergistically amplified nitric oxide production, TNFα release, and DA neurotoxicity. This association is crucial for Mexico City (MC) young residents (Calderón-Garcidueñas et al., 2009a, 2009b, Rosas Pérez et al., 2007; Querol et al., 2008; Vega et al., 2011), since endotoxins (LPS) are an important organic particle component and *healthy* children show an endotoxin tolerance-like state (Calderón-Garcidueñas et al., 2009a, 2009b).

We recently documented by magnetometry, high-resolution transmission electron microscopy (HRTEM), electron energy loss spectroscopy (EELS), and energy dispersive X-ray (EDX) analysis the mineralogy, morphology, and composition of magnetic frontal cortex NPs from MC young residents (Maher et al., 2016) and used transmission electron microscopy to identify combustion-derived nanoparticles (CDNPs) in neurons, glia, choroid plexus, and neurovascular units of MC young residents v matched clean air controls (González-Maciel et al., 2017). CDNPs are spherical nanoparticles associated with pathology in mitochondria, endoplasmic reticulum (ER), mitochondria-ER contacts (MERCs), axons and dendrites. We commented that abnormal MERCs, mitochondria and dilated ER are widespread in brain tissues and CDNPs in close contact with neurofilaments, glial fibers and chromatin are a potential source for altered microtubule dynamics, mitochondrial dysfunction, accumulation and aggregation of unfolded proteins, abnormal endosomal systems, altered insulin signaling, calcium homeostasis, apoptotic signaling, autophagy and epigenetic changes (González-Maciel et al., 2017).

We are very concerned about the passage of NPs through damaged cell junctions in small bowel and the fact MC children have higher levels of antibodies to host proteins involved in cell adhesion (Calderón-Garcidueñas et al., 2015a, 2015b, 2015c, 2015d). MC children and young adults are already showing Parkinsons' disease early neuropathological hallmarks, including accumulation of alpha synuclein in olfactory bulb and brainstem (Calderón-Garcidueñas et al., 2008, 2010, 2013a, 2016a, 2016b, 2016c). Kish and colleagues work is key given the increased gut permeability in mice exposed to particulate matter with a diameter of < 10 μm (PM_{10}) and their conclusions of ingestion of airborne particulate matter altering the gut microbiome and inducing acute and chronic inflammatory responses in the intestine (Kish et al., 2013).

At the core of our work Braak and Del Tredeci proposals (Braak et al., 2003a, 2003b; Tredici and Braak, 2016) "*a putative environmental pathogen capable of passing the gastric epithelial lining might induce α-synuclein misfolding and aggregation*" and the dual-hit hypothesis of Hawkes (Hawkes et al., 2007), both fit the strong possibility *putative environmental pathogens* are indeed swallowed nanoparticles gaining access to the brain through the most vulnerable section of the GI tract: the small bowel (Johansson et al., 2013).

Given that MC children have lifetime exposures to high concentrations of $PM_{2.5}$ and well documented breakdown of epithelial, endothelial and neurovascular barriers (Calderón-Garcidueñas et al., 2008, 2012, 2016a, 2016b, 2016c), and having the experience of studying healthy dogs exposed to the same environment as the children (Calderón-Garcidueñas et al., 2001, 2009a, 2009b), we hypothesized that healthy MC facility dogs will have NPs in the neuroenteric system and similar findings could be seen in children and young MC adults.

There were three primary aims to this study: 1. To study by electron microscopy the integrity of the small bowel epithelium tight junctions, the endothelial barrier and the passage of NPs from circulating red blood cells loaded with particles in blood vessels to the intestinal compartments, 2. To identify and measure NPs and document organelle pathology in the neuroenteric system including the submucosal and myenteric plexus fibers and neurons in duodenal, jejunum and ileum samples of healthy young residents in MC versus controls 3. Since the vagus nerves play a key role in the early neuropathology of PD, we specifically sampled right cervical vagal (X) samples both in dogs and in human autopsies (human samples previously analyzed for mRNA COX2, IL1β and CD14 and found to have high levels versus clean air controls (Calderón-Garcidueñas et al., 2008). Given that highly exposed children and young adults have early features of Parkinson's and Alzheimer diseases (Calderón-Garcidueñas et al., 2008, 2010, 2011, 2012, 2016c, 2017), we did immunohistochemistry for phosphorylated α-synuclein and hyperphosphorylated tau in gastric and vagal samples for the same subjects with right vagal mRNA inflammatory markers (Calderón-Garcidueñas et al., 2008).

Our results identify abnormalities in the apical junctional complexes, desmosomal and gap junctions resulting in interepithelial gaps in the small bowel of MC dogs, along with increased caveolar activity in the luminal and abluminal endothelial cells versus controls. Airborne iron-rich strongly magnetic combustion-derived nanoparticles (CDNPs) are abundant in epithelial and endothelial cells and in enteric neurons, unmyelinated axons and cervical X nerves of MC children and young adults and are associated with pathology in mitochondria, axons and dendrites. Gastric accumulation of hyperphosphorilated α-synuclein (α-Syn) and P-tau is a key finding. Our study shows urban young residents have α-Syn and P-tau pathology of the enteric nervous system and neuronal, axonal and unmyelinated pathology. Combustion-derived nanoparticles likely play a key role in the breakdown of the GI barrier and the α-syn/P-tau neuroenteric pathology. Exposures to CDNPs ought to be contemplated as Parkinson's and Alzheimer's environmental risk factors (Calderón-Garcidueñas et al., 2008, 2010, 2011, 2012, 2016a, 2016b, 2016c, 2017; Maher et al., 2016).

2. Materials and methods

2.1. Study cities and air quality

Mexico City is a prime example of uncontrolled urban growth and sustained severe air pollution (Rosas Pérez et al., 2007; Querol et al., 2008; Vega et al., 2011; Secretaria del Medio Ambiente, 2012, 2012). Driving restriction programs implemented in 2017 have failed to improve air quality (Davis, 2017). The metropolitan area of over 2000 km^2 lies in an elevated basin 2200 m above sea level surrounded on three sides by mountain ridges. MC Metropolitan area nearly 24 million inhabitants, over 50,000 industries, and 5.5 million vehicles consume more than 50 million liters of petroleum fuels *per day*. Northern MC residents have been exposed to higher concentrations of volatile and toxic organic compounds, PM_{10}, and $PM_{2.5}$ including high levels of its constituents: organic and elemental carbon, nitro- and polycyclic aromatic hydrocarbons and metals (Zn, Cu, Pb, Ti, Mn, Sn, V, Ba), while southern residents (exposed dogs in this study are from SW Mexico City) have been exposed continuously to significant and prolonged concentrations of ozone, secondary aerosols (NO_3^-) and particulate matter associated with lipopolysaccharide PM-LPS (Rosas Pérez et al., 2007; Querol et al., 2008; Vega et al., 2011). Studies on the composition of $PM_{2.5}$ with regards to sites and samples collected in 1997 show that composition has not changed during the last decade. Tlaxcala was the selected clean air control with criteria air pollutants typically below the equivalent US EPA air quality standards (Calderón-Garcidueñas et al., 2009a, 2009b).

2.2. Dog small bowel and vagus samples

Previously harvested dog small bowel and right vagus samples for electron microscopy were used for this study (Calderón-Garcidueñas et al., 2009a, 2009b, 2016a, 2016b, 2016c). MC and control mixed beagles were whelped and housed in an outdoor-indoor kennel; husbandry was in compliance with the American Association of Laboratory Animal Certification Standards. Dogs were under daily veterinarian

observation during their entire life, and at no time there was any evidence of respiratory, cardiovascular, gastrointestinal or neurological diseases. Dogs had all applicable vaccines and were treated with antihelmintics regularly. Dogs from both cohorts had the same diets. We selected to use small bowel and cervical vagus nerves optimally fixed electron microscopy samples from 6 dogs (5.1 ± 1.7 years) from an independent longitudinal study involving the use of Nimesulide® in mixed beagle dogs. The 6 selected dogs for this study were in the non-treated Mexico City dog group exposed 24/7 to the Southwest MC atmosphere from birth. Four dogs average age 4.6 ± 2.4 years from Tlaxcala, the selected control city were also studied. Procedures used were in accordance with the guidelines of the Use and Care of Laboratory Animals (NIH Pub no. 86-23).

2.3. Children and young adult small bowel, gastric and vagus samples

Children and young adult autopsy tissue MC and control vagal samples in this study have been previously studied (Calderón-Garcidueñas et al., 2008). Subjects were clinically healthy before sudden accidental deaths, were APOE and TLR4 (Asp299Gly) genotyped and had full autopsies, including complete neuropathological examinations. Thirty-six gastric and right cervical vagus samples for immunohistochemistry (IHC) were studied from 27 MC and 9 controls subjects (Calderón-Garcidueñas et al., 2008). The average age of MC subjects was 24.03 ± 10.5years (8 children 12.5 ± 5.12 y) and controls had an average age of 21.3 ± 10.3 y (4 children 13.2 ± 7.5 y) (Supplementary Tables 1 and 2).

2.4. Children and young adult vagus samples for electron microscopy

We selected 18 right cervical vagus samples including 5 controls average age 17.4 ± 9.65 years and 13 Mexico City residents average age 24.7 ± 12.2 years (Supplementary Tables 1 and 2).

2.5. Light microscopy

The hematoxylin-eosin slides from the entire autopsy were reviewed to rule out a disease process that will interfere with the final evaluation of the GI and vagal tissues. Sections 1 μm thick were cut and stained with toluidine blue in preparation for the selection of electron microscopy samples. Board-certified anatomical pathologist/neuropathologists and Electron Microscopy researchers without access to the identification codes reviewed the sections.

2.6. Immunohistochemistry

Specimens for IHC were kept in 10% buffered formaldehyde ranging from 24 h to 1 week. Six micrometer-thick sections were cut from paraffin-embedded tissue blocks. IHC specimens included stomach and right cervical vagus. IHC was performed using a primary antibody from alpha-synuclein phosphorylated at Ser-129 LB509 (In Vitrogen, Carlsbad, CA 1:800) and p-tau using mouse monoclonal antibody AT8 pSer202/Thr205 2:1000 (Thermo Scientific, Rockford,IL,US) with pretreatment conditions with formic acid 88% for 10 min. Detection of immunostaining was performed using the ImmPRESS peroxidase universal MP-7500 (Vector Laboratories, Burlingame, CA) and diaminobenzidine DakoCytomation K3468 (Dako, Carpinteria, CA) or HIGHDEF ® Red IHC Chromogen (ENZO, Farmingdale,NY) were used as chromogens. Control of antibody specificity included omission of the primary antibody or preabsortion of the antibody with full length recombinant alpha synuclein, A53T (rPeptide S-1002). Sections were mounted with a commercial aqueous mounting media, coverslipped, and dried overnight before nail polishing the edges to seal. Blind assessment of α-Syn and P-tau immunoreactivity (IR) was performed and the immunostaining pattern, intensity and cellular location evaluated. For a given tissue sample, 6–10 levels were examined and the positive stain was assessed semiquantitatively following an arbitrary grading system: - no lesions, + 1–10 at × 200 magnification; + + 11–20 positive areas per field and + + + > 21 areas per field. The data on the positive density collected in each subject was averaged.

2.7. Examination of small bowel samples by Transmission Electron Microscopy (TEM)

Tissues were post-fixed in 1% osmium tetraoxide and embedded in Epon. Semi-thin sections 0.5–1 μm) were cut and stained with toluidine blue for light microscopic examination. Ultra-thin sections (60–90 nm) were cut and collected on slot grids previously covered with formvar membrane. Sections were stained with uranyl acetate and lead citrate and examined with a JEM-1011 (Japan) microscope. Each electron micrograph was evaluated separately, then compared by group. We identified the type of cell and captured the ultrastructural characteristics of the cells including ganglionic submucosal and muscularis neurons and submucosal plexus, and their organelles. We captured TJ's complexes, measured the diameter of the nanoparticles present in epithelium, umyelinated axons, and neurons and describe the abnormal organelles and their relationship with NPs. One EM researcher with ample experience examined all sections at magnifications between 5000 × and 120,000 × and took representative pictures. For the purpose of measuring NPs, pictures were taken at various magnifications including 60,000 with print magnifications at 85,000 × 7"; 25,000 with print magnifications at 41,600 × 8"; 50,000 × with prints 83,300 × 8"; 80,000 × with prints 117,000 × 7" and 80,000 × with prints 133,000 × 8". We counted particles in ganglionic neurons (cytoplasm, mitochondria and nucleus) from duodenal and jejunal dog samples MC versus controls and the results were based on the evaluation of 8 ± 2 pictures per case assessed for significance with a p test after adjusting for age.

2.8. Examination of vagus samples by Transmission Electron Microscopy (TEM)

Tissues were post-fixed in 1% osmium tetraoxide and embedded in Epon. Sections were stained with uranyl acetate and lead citrate, and examined with a JEM-1011 (Japan) microscope. Each case was blindly evaluated separately, then compared by group. We captured the ultrastructural characteristics of the axons and ganglionic and satellite cells and their organelles. For the purpose of measuring NPs, we followed the same protocol as for small bowel samples.

2.9. Statistical analysis

We first calculated the mean and standard deviations (SD) of all variables in all locations. Then, we carried out statistical tests for the differences between the measurements of the variables in Mexico City and low pollution controls. We used regression techniques to accomplish this. Then, we performed two sample *t*-tests for testing the differences between NPs types, numbers and/or diameters in dogs and human samples in Mexico City and low pollution controls. Statistical analyses were carried out using Excel and R (https://www.r-project.org/).

3. Results

3.1. Air quality data

Mexico City residents are exposed year-round to $PM_{2.5}$ concentrations above United States National Air Ambient Quality Standards (NAAQS). The $PM_{2.5}$ annual air quality standard of 12 $\mu g/m^3$ has been historically exceeded across the metropolitan area. We are focused on fine and ultrafine particulate matter (PM), broadly defined by the diameter of the aerodynamic particles: fine particles (< 2.5 μm, $PM_{2.5}$)

Table 1
Data on Mexico City and low pollution control dogs, including the number of NPs counted on submucosal ganglionic neurons mitochondria, nucleus and cytoplasm.

Dogs residency	Number/Gender	Age	Cytoplasm	Mitochondria	Nucleus
Control City	2F/3M	4.6 ± 2.4 years	9.2 ± 2.7	9.8 ± 2.5	10.6 ± 2.6
Mexico City	2F/4M	5.1 ± 1.7 years	25.5 ± 4.8	26.5 ± 6.9	33.6 ± 13.3
p values adjusted for age			< 0.0001	< 0.0001	< 0.0001

and ultrafine PM (UFPM < 100 nm) (Querol et al., 2008; Vega et al., 2011; Molina et al., 2010). Ultrafine PM is of particular interest given their capability to reach the brain and produced extensive damage (Maher et al., 2016; González-Maciel et al., 2017). MC children in this study have been exposed to significant concentrations of $PM_{2.5}$ during their entire life, including the prenatal period. The high concentrations of $PM_{2.5}$ coincide with the time children play outdoors and/or stay in schools with broken windows and doors. Control dogs and humans have been lifelong residents in low pollution cities with all criteria air pollutants below the US EPA NAAQS standards.

3.2. Measurement of NPs in mitochondria, nuclei, and free in the cytoplasm in enteric ganglionic neurons from dogs' samples

We distinguished spherical combustion-derived nanoparticles consistent with high temperature formation versus euhedral particles ascribed to endogenous sources based on Maher et al. (2016) paper. The numbers of NPs were significant higher in the exposed subjects (Table 1), the percentage of CDNPs versus euhedral NPs was 37–63% across the epithelial, endothelial and axonal/dendritic samples, while the vagus samples showed 44–56% with a predominance of endogenous NPs. Table 2A shows the average size nanoparticles for the different compartments analysed and in Table 2B the data for the vagus nerves in dogs and humans. There were significant differences in sizes of CDNPs v euhedral NPs in Mexico City enteric neurons samples ($p < 0.0001$), while controls showed no differences (Table 2A). The vagal samples from both dogs and humans showed significant differences in the sizes of CDNPs v euhedral NPs in both controls and exposed subjects. The smallest CDNPs were seen in human vagal samples (Table 2B).

3.3. Electron microscopic results

3.3.1. Dogs' small bowel samples

Toluidine blue 1 μm sections of normal duodenal epithelium with an intact brush zone and unremarkable enterocytes and goblet cells is characteristic of the control dogs (Fig. 1A). Highly exposed dogs exhibited duodenal samples with severely disrupted epithelial lining, breakdown of the barrier with numerous epithelial cells gaps and abundant cell debri (Fig. 1B, C). Electromicrographs of jejunum in MC dogs show numerous nanoparticles associated with villae and distributed across the enterocytes' cytoplasm and abnormal tight junctions (Fig. 2A–C). Clusters of compact aggregates of neurons (ganglion cells), Schwann cells, glial-like cells, and/or unmyelinated axons are seen throughout the small bowel walls as components of the submucosal plexus and the myenteric plexus. The myenteric plexus between the longitudinal and circular layers of muscularis externa in the small bowel of MC dogs is surrounded by connective tissue bands and vascular elements (Fig. 3A). Schwann cells and umyelinated fibers alike contain numerous NPs and abnormal axons are a common finding (Fig. 3B, C). Lipofuscin is seen in Schwann and neurons' cytoplasm in very young subjects (Fig. 3D), fibers with a diameter ranging between 7.1 and 13.5 nm are seen inside and outside neurons (Fig. 3E),and numerous abnormal unmyelinated axons without defined organelles contain NPs (Fig. 3F). Ganglion cells, Schwann cells and clusters of abnormal unmyelinated axons share the presence of combustion-derived NPs (Fig. 4). The close proximity between abundant submucosal capillaries with red blood cells loaded with NPs, increased abluminal caveolar endothelial activity and unmyelinated axons poise the potential transfer of NPs from capillaries to the numerous unmyelinated axons (Fig. 5). Both CDNPs and euhedral NPs are seen in unmyelinated axons and presynaptic axons and dendrites (Fig. 6). CDNPs are also seen free in the interstitial space surrounded by collagen fibers and in close proximity to isolated individual filaments (Fig. 7). Smooth muscle cells and endothelial cells also exhibit numerous CDNPs in their damaged organelles (Fig. 8). Transfer of nanoparticles is a common finding in highly exposed dogs, the transfer takes place between luminal red blood cells to endothelial cells in the small bowel capillary network (Fig. 9). Interestingly, numerous endothelial cell fragments with no visible attachment to the endothelial cell contain CDNPs (Fig. 9B). Vagus dog and human samples show abundant CDNPs in axonal mitochondria, and in clusters of laminar ill-defined structures (Fig. 10). Extensive and severe mitochondrial damage is common and focal myelin fragmentation is seen in highly exposed subjects (Fig. 10). Cervical vagus nerves 1 μm toluidine blue sections show small clusters of thinly myelinated axons alternating with larger myelinated fibers (Fig. 11A, B). There is no evidence of inflammatory cells. A-Syn IR was seen in highly exposed young humans and distinct punctate cytoplasmic staining of ganglion cells (Fig. 11C and D). Positive A-Syn fibers were seen in cervical vagus samples (Fig. 11D). Large, coarse aggregates of α-Syn were not observed in the vagus nerves.

Gastric samples (Fig. 12) showed two basic IR patterns with hyperphosphorilated α-Syn: a distinct punctate cytoplasmic staining of ganglion cells and strongly positive coarse cytoplasmic aggregates in cells distributed widely through the submucosa and the muscularis (Fig. 12A, B). Clear cut positive coarse neurites could be seen in each positive case (Fig. 12B insert)and ganglion cells exhibited coarse positive neurites(Fig. 12C). Clean air controls were negative (Fig. 12D). Hyperphosphorilated tau IR (Fig. 13) was extensively distributed throughout the gastric submucosa, muscularis mucosae and ganglion cells. Both delicate (Fig. 13A, B) and coarse (Fig. 13C, D) positive

Table 2A
Average size of nanoparticles (combustion-derived and endogenous euhedral) in small bowel epithelium, enteric neurons and unmyelinated axons in Mexico City and low pollution control dogs.

Tissue	CTL CDNP	CTL Euhedral NPs	p values paired *t*-test	MC CDNP	MC Euhedral NPs	p values paired *t*-test
Small bowel epithelium	**11.57 ± 4.68[a]**	**12.4 ± 5.6**	**0.46**	**11.33 ± 3.96[a]**	**12.43 ± 4.3**	**0.19**
Unmyelinated Axons	**15.29 ± 6.63[*]**	**20.41 ± 10.23**	**0.002**	**21.99 ± 10.8[*]**	**17.91 ± 8.9**	**0.06**
Enteric neurons	**16.9 ± 8.1[a]**	**20.4 ± 9.53**	**0.09**	**15.42 ± 6.01[a]**	**21.27 ± 9.0**	**< 0.0001**

[*] < 0.0001.
[a] NS.

Table 2B
Cervical vagus electron microscopy data: average size of nanoparticles (combustion-derived and endogenous euhedral) in cervical right vagus nerves in Mexico City and low pollution control dogs and humans.

X cervical	CTL CDNP	CTL Euhedral NPs	p values paired *t*-test	MC CDNP	MC Euhedral NPs	p values paired *t*-test
Vagus dogs CTL n:4 MC n:6	13.04 ± 5.66[a]	27.85 ± 16.59	< 0.0001	12.06 ± 4.75[a]	35.38 ± 27.48[*]	< 0.0001
Vagus humans CTL n:5 MC n:13	11.97 ± 4.34[a]	17.14 ± 8.02	0.0008	11.85 ± 4.03[a]	18.4 ± 8.27[*]	< 0.0001

[a] NS.
[*] < 0.0001.

neurites were seen and extensive number of positive fibers were seen in association with ganglion cells (Fig. 13D). Positive fine synaptic-type staining of muscular plates were also observed (Fig. 13B). The results of IR for α-Syn and Htau in gastric and vagal samples with the ages, gender and APOE and TLR4 (Asp299Gly) genotyping results are shown in Supplementary Tables 1 and 2.

4. Discussion

The integrity of the gastrointestinal (GI) epithelial, endothelial and neuroenteric structures is compromised in dogs, children and young adults residents in Mexico City. The enteric nervous system (ENS), a network of neurons and glia that controls GI functions shows significant pathology in key organelles and aggregated hyperphosphorilated α-synuclein and P-tau adds to the neuropathological findings of Braak stages 1 and II Parkinson disease already described in similar cohorts in Mexico City children and young adults (Calderón-Garcidueñas et al., 2008, 2010, 2013a, 2013b). The passage of NPs through the damaged GI epithelial barrier and the transfer of NPs from the RBC in circulation to the capillary GI network likely gives rise to inflammatory and immune responses triggered to prevent injury to the ENS and underlying structures (Chow et al., 2017).

Compromising the integrity of the small bowel tight junctions (Calderón-Garcidueñas et al., 2015a, 2015c), likely alters its physiology and function (Volk and Lacy, 2017; Chow et al., 2017) and translates in a disrupted GI barrier that will allow for major concentrations of swallowed PM entering the neuroenteric components, reaching the vagus nerves and the brainstem. Particulate matter is in fact gaining access through the most vulnerable section of the GI tract: the small bowel (Kish et al., 2013; Johansson et al., 2013), and microbial translocation, immune alterations and a dysbalanced brain-gut axis are fully expected (Ermund et al., 2013; Douglas-Escobar et al., 2013; Bonazzi and Cossart, 2011; Klatt et al., 2010; Vuong et al., 2017; Yang et al., 2017).

The organelle damage to GI neuroenteric components and the presence of the two key abnormal proteins associated with Parkinson and Alzheimer's diseases in highly combustion-derived particulate matter exposed subjects showing cognitive and olfactory deficits and autonomic symptomatology (Calderón-Garcidueñas et al., 2010, 2013a, 2013b, 2016a, 2016b, 2016c, 2017) is at the core of this discussion. Ultrafine and fine PM produced by combustion products is composed of organic and inorganic components, including iron-rich magnetic nanoparticles, heavy metals, volatile organic compounds, and endotoxins, and because of their high and very effective pro-oxidative potential and their inflammatory capacity, their risk for neurotoxicity is high (Rosas Pérez et al., 2007; Querol et al., 2008; Vega et al., 2011; Bergin and

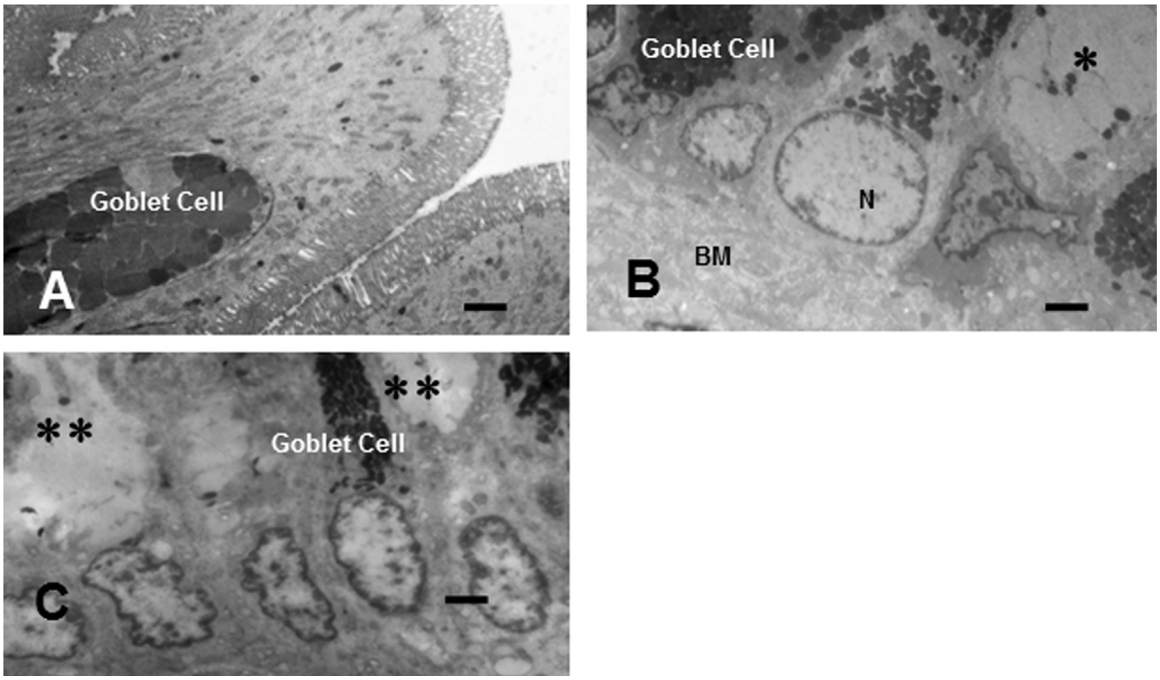

Fig. 1. A. Four year old Tlaxcala, clean air dog, the duodenal epithelium show a normal, columnar epithelium with goblet cells alternating with enterocytes. Scale bar: 2 μm. B. Matched Mexico City dog with an abnormal duodenal epithelium, the brush border is not visible and focal areas of epithelium exhibit breakdown with wide gaps (*), goblet cells are numerous. Scale bar: 2 μm. C. Same dog as in B with extensive breakdown (**) of the epithelial surface. Scale bar: 2 μm.

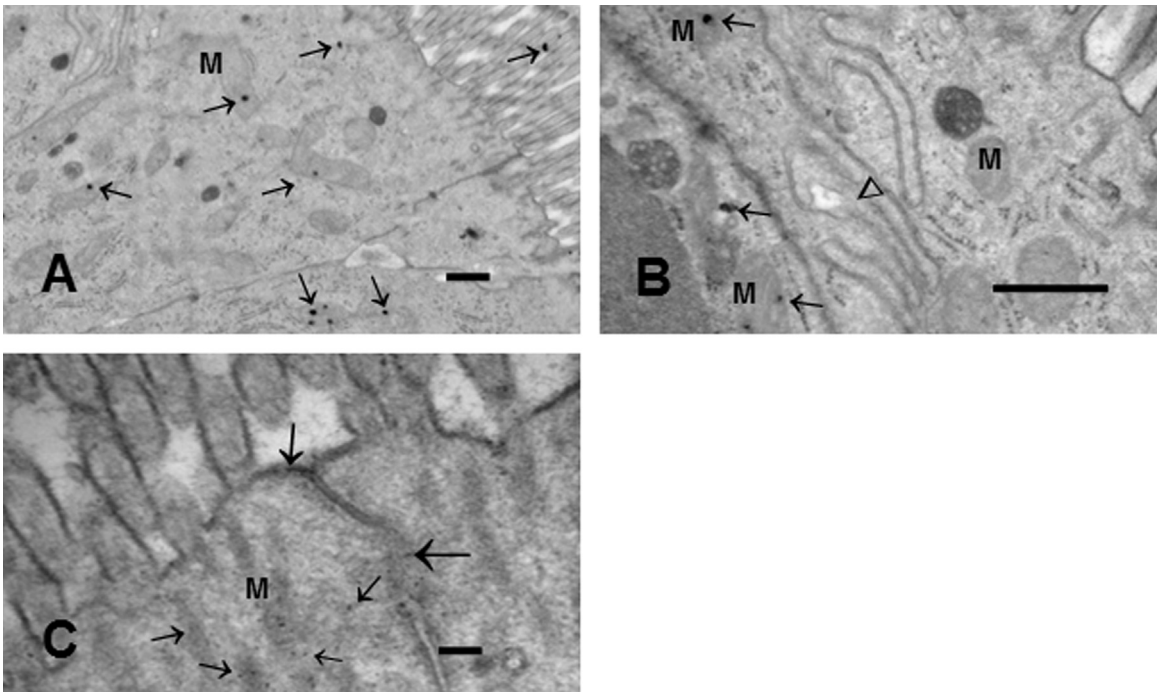

Fig. 2. A. Jejunal epithelium from a 3 y old MC clinically healthy dog shows spherical combustion-derived nanoparticles in the brush border (superior arrow). Numerous nanoparticles are seen throughout the cytoplasm both free (arrows) and within mitochondria (M). Scale bar: 2 μm. B. There is a breakdown of the intercellular spaces (arrow head) and mitochondria exhibit numerous NPs (long arrows). Scale bar: 500 nm. C. A cluster of abnormal mitochondria (M) adjacent to the villous border is characterized by conglomerates of NPs (short arrows). The upper arrow between the cells points to junctional complexes between two enterocytes, with clusters of NPs, while the larger arrow points to a segmental discontinuity of a zonula adherens. Scale bar: 100 nm.

Witzmann, 2013; Yu et al., 2013; Gehr et al., 2011).

The presence of aggregated alpha synuclein in olfactory bulbs, brainstem, GI tract and vagus nerves in MC young residents signpost the early stages Parkinson's disease (Calderón-Garcidueñas et al., 2013a, 2013b). The association between nanoparticles and the kinetics of α-synuclein aggregation is therefore very relevant for megacity residents (Xie and Wu, 2016; Fink, 2006; Rodriguez et al., 2015; Alvarez et al., 2013; Harischandra et al., 2017; Phukan et al., 2016; Corbillé et al., 2017). Different types of NPs induce oxidative stress, autophagy, reduction of proteasome activity, and amyloid aggregates of α-synuclein in dopaminergic neurons of the midbrain (Phukan et al., 2016; Hu et al., 2017; Xie and Wu, 2016; Xie et al., 2016). Of particular interest is the work of Harischandra and colleagues (Harischandra et al., 2017) because manganese, an environmental neurotoxicant present in high concentrations in frontal cortex of MC young residents (Calderón-Garcidueñas et al., 2013a, 2013b) induces cytotoxicity in a MN9D dopaminergic cell model of PD. Specifically, Harischandra's group demonstrated Mn exposure (300 μM $MnCl_2$) for 24 h modulated extracellular miRNA content through exosomal release from dopaminergic neuronal cells, potentially contributing to progressive neurodegeneration. Further, miRNA profiling analysis showed increased expression of miRNAs shown to regulate protein aggregation, autophagy, inflammation and hypoxia. This is very relevant to our findings in children and young MC adults where indices of neuroinflammation, oxidative stress, dysregulation of IL1, NFκB, TNF, IFN, TLRs and PrP(C) relate to their environmental exposures including particulate matter and heavy metals (Calderón-Garcidueñas et al., 2008, 2012). Metallothioneins (MTs) proteins that function by metal exchange to regulate the bioavailability of metals, also are likely to play a role in the binding and aggregation of alpha-synuclein (Okita et al., 2017).

The association between neuronal and axonal abnormal mitochondria and CDNPs present among the abnormal cristae and in the mitochondria membranes bring the issue of serious damage to an organelle needed for the high energy neuronal and axonal requirements (Giannoccaro et al., 2017; Erpapazoglou et al., 2017; Scott et al., 2017). As described by Giannoccaro and coworkers, damage to mitochondria will alter its complex homeostatic functions, their dynamic fission/fusion cycles, the balance of mitobiogenesis and mitophagy, and consequently the quality control surveillance that corrects faulty mitochondrial DNA maintenance, all key in the pathogenesis of PD (Giannoccaro et al., 2017). Iron oxide NPs are particularly cytotoxic and generate membrane leakage, intracellular reactive oxygen species and mitochondrial damage (Dönmez Güngüneş et al., 2017). Equally relevant to the neuroenteric system is the interaction of the NPs with the extracellular matrix, cell membranes and cytoplasm of other cells (i.e., glial) (Lindström et al., 2017), that may be affected by the agglomeration behavior of the NPs, their degree of mobility and internalization. In the work of Dönmez Güngüneş et al., Fe_3O_4 NPs show superparamagnetic behavior leading to intense aggregation (Dönmez Güngüneş et al., 2017), an observation we have made in the cervical vagal (X) human nerves (Fig. 10E). The agglomeration, common for NPs (as most of them have surface charges which interact with the cell and form protein coronas) may prevent NPs from membrane permeation (Dönmez Güngüneş et al., 2017). ROS generation representing oxidative stress is key in the mitochondrial effects of NPs, which overcomes the antioxidant ability of the cell and induces mitochondrial dysfunction (Xie et al., 2016). Xie et al. (2016) clearly demonstrated that the size of the magnetic iron oxide (Fe3O4) NPs were significant for the type of damage inflicted upon mitochondria using human hepatoma cells: 9 nm magnetic iron oxide particles produced ROS generation and the resultant mitochondrial dysfunction and necrosis, while 14 nm NPs damaged the plasma membrane and give rise to massive lactate dehydrogenase leakage (Xie et al., 2016). Moreover, the authors also showed that agglomerated 9 nm NPs resulted in severe oxidative stress and a combination of necrosis/apoptosis. The diameter of the CDNPs is likely a key issue for the neuroenteric system, the average size combustion-derived NPs in the human enteric neurons and vagus nerves for example was 12.06 ± 4.7 nm, significantly smaller that similar particles in the brain (29.17 ± 11.22 nm) and CSF (51.89 ± 12.95 nm) (González-Maciel et al., 2017). The issue is critical

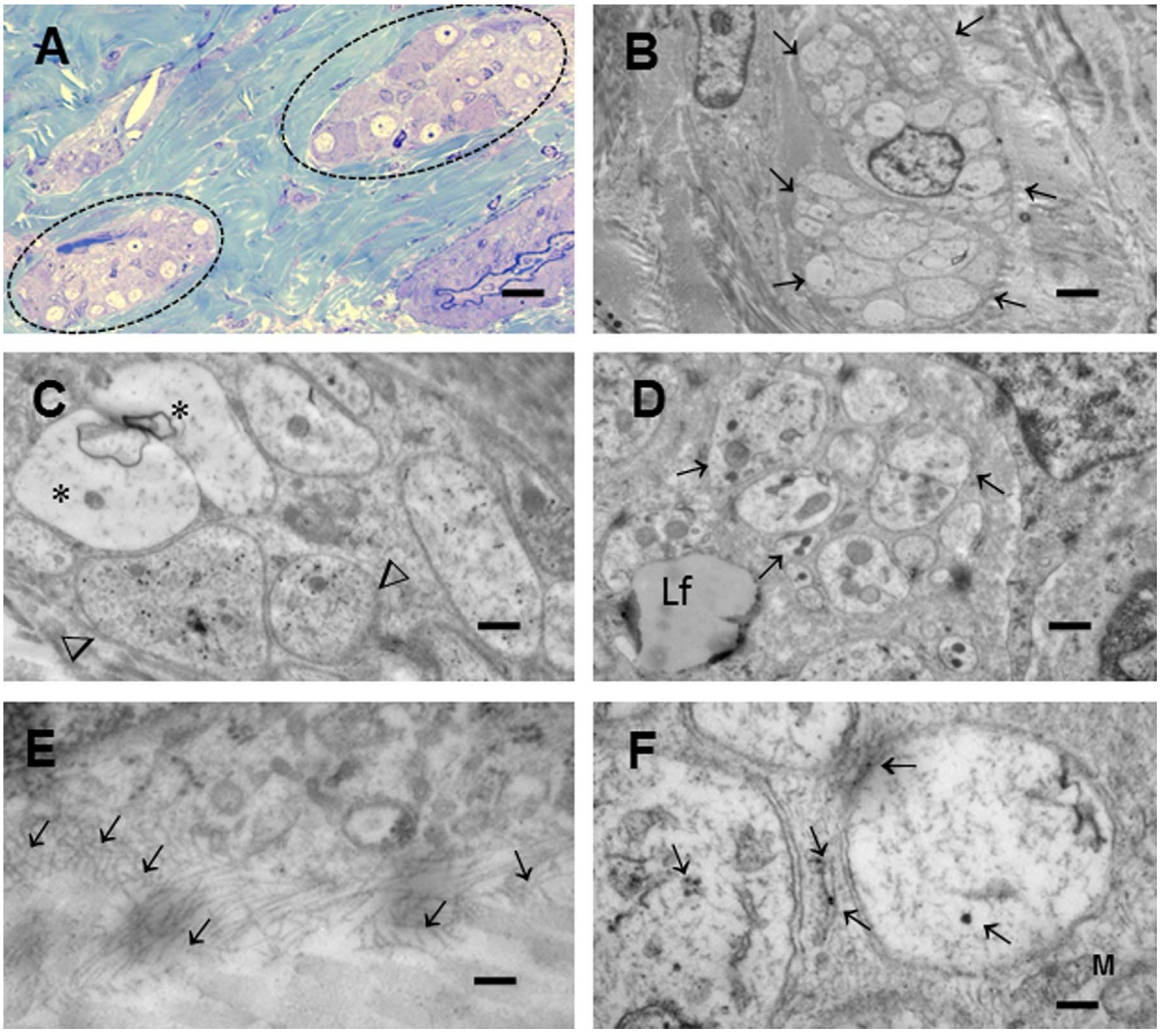

Fig. 3. A. Toluidine blue 1 μm section of a cluster of ganglionic cells in submucosal region of duodenum. Abundant fibrous connective tissue (blue) surrounds two marked ganglion cells clusters and axons.Scale bar: 20 μm. B. TEM from a 4 y old MC dog showing a cluster of unmyelinated axons and the nucleus of a Schwann cell (arrows mark the cluster). Scale bar: 2 μm. C. There are 7 unmyelinated axons, the vacuolated, degenerated ones are marked with *, while the remaining axons show numerous NPs. Scale bar: 500 nm. D. Lipofuscin (Lf) granules are a common finding in all types of neural cells (as in this Schwann cell) even in young subjects, like this 1 year MC dog. Scale bar: 500 nm. E. This is a ganglionic submucosal cell with abundant fibers with a size range of 7.1–13.5 nm, their location is not well defined and apparently are located in and outside of the cell borders. These fibers are similar in size to α-Syn. Scale bar: 100 nm. F. Several unmyelinated axons with various degrees of neurodegeneration are seen. The two right arrows point to NPs inside the axon and in the bilaminar membrane. Scale bar: 100 nm. (For interpretation of the references to color in this figure legend, the reader is referred to the web version of this article.)

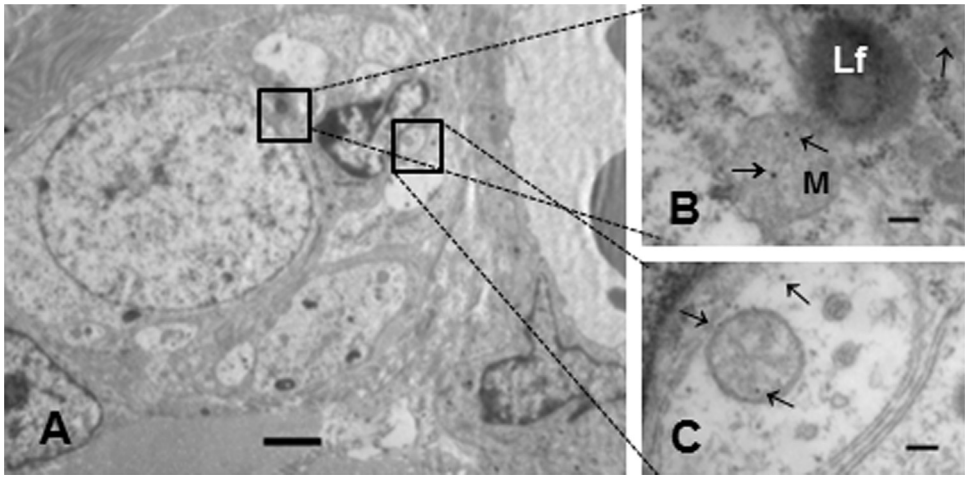

Fig. 4. A. ganglionic neuron and a Schwann cell with a cluster of unmyelinated axons adjacent to a blood vessel. Scale bar: 2 μm. Two areas are squared for higher magnifications: B, a neuron cytoplasmic area in close proximity to the Schwann cell cytoplasm and in C a portion of the Schwann cell cytoplasm. B. Two structures are at the center of this picture: one mitochondria on the neuronal side showing two distinct nanoparticles and a lipofuscin structure on the Schwann cell side. This is a 1 year old dog and lipofuscin is not expected. Scale bar: 100 nm. C. The unmyelinated axon within the Schwann cell cytoplasm display a mitochondria with NPs (arrows mark the NPs). Scale bar: 100 nm.

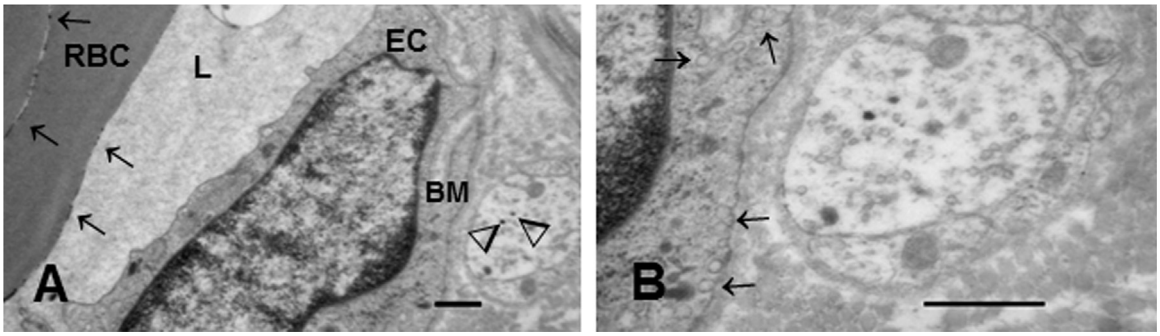

Fig. 5. A. One capillary in the submucosal region of the duodenum of a 2 year old Mexico City dog. The lumen is occupied by 2 red blood cells showing NPs, the endothelial cell is marked EC and the vessel lumen L. Notice the small unmyelinated axon with 2 NPs (two head arrows) to the right side of the endothelial basement membrane (BM). Scale bar: 500 nm. B. A higher power of the unmyelinated axon in A. There is a brisk caveolar activity in the subluminal region of the endothelial cell (arrows). Please notice the proximity of the increased caveolar activity with traffic of NPs with the axon and the presence of CDNPs in the axoplasm. Scale bar: 500 nm.

because Alvarez and colleagues (Alvarez et al., 2013) have shown gold nanoparticles produced a strong acceleration of α-synuclein aggregation depending on the size and concentration of the nanoparticles, being strongest for NPs 10 nm in diameter, which produced a 3-fold increase in the overall aggregation rate at concentrations as low as 20 nM. Damage to lysosomal and mitochondrial structures at lower NPs concentrations that concentrations producing disruption of plasma membranes are also described (Bermejo-Nogales et al., 2016). In their work, at non detectable cytotoxic concentrations, the silver NPs persisted inside nucleoli and mitochondria, raising the issue of direct effect to these critical organelles with time. Hyperphosphorilated alpha-synuclein, mitochondrial dysfunction, inability of cells to regulate Ca^{2+} and neurodegeneration have been discussed in the NPs and the PD literature (Dönmez Güngüneş et al., 2017; Erpapazoglou et al., 2017; Rocha et al., 2017; Zaichick et al., 2017).

The architecture of parasympathetic axons innervating the GI tract is key knowledge to understand the potential axonal transport of NPs from the GI tract to the brain (McMenamin et al., 2016; Uesaka et al., 2016; Ting et al., 2017; Walter et al., 2016; Powley et al., 2016). The GI tract gets innervation from sympathetic and parasympathetic nervous systems, which regulate and modulate the function of the enteric nervous system (McMenamin et al., 2016). The ENS consists of two main ganglionated layers: myenteric and submucosal ganglia, containing enteric neurons and glial cells (Uesaka et al., 2016). ENS cells are mostly derived from vagal neural crest cells (NCCs), which proliferate, colonize the entire gut, and first populate the myenteric region (Uesaka et al., 2016). After gut colonization by vagal NCCs, the extrinsic nerve fibers reach the GI tract, and Schwann cell precursors (SCPs) enter the gut along the extrinsic nerves (Uesaka et al., 2016). Vagal endings are abundant around the celiac ganglion neurons, and the right is usually the one with the most endings. As discussed by McMenamin and collaborators, the stomach and small bowel are heavily influenced by the parasympathetic nervous system (vagus nerve) and disruption of vagal sensory or motor functions translates in disorganized motility patterns, disrupted receptive relaxation and accommodation, and delayed gastric emptying (all non-motor symptoms of PD) (McMenamin et al., 2016; Doty, 2012; Massano and Bhatia, 2012; Liu et al., 2017). The issue of transport of NPs from the GI tract to the brain is relevant because Braak et al. proposal (Braak et al., 2003a, 2003b) "*a putative environmental pathogen capable of passing the gastric epithelial lining might induce α-*

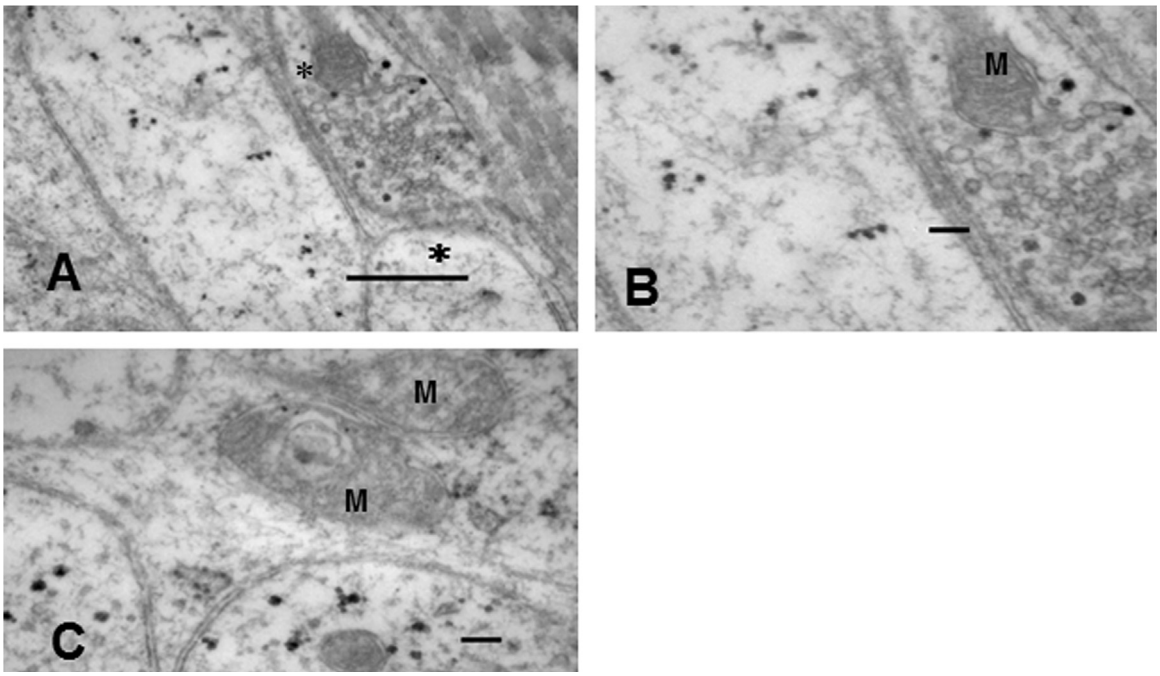

Fig. 6. Unmyelinated axons with numerous NPs from exposed MC dogs. A and B Unmyelinated presynaptic and postsynaptic axons. The presynaptic one at a higher power in B shows numerous synaptic vesicles and a mitochondria. Numerous CDNPs are seen in both the presynaptic and the postsynaptic axons. Scale bar: 500 nm. C Numerous CDNPs of different sizes (arrows) in the axoplasm of every axon. The mitochondria (M) have abnormal cristae. Scale bar: 100 nm.

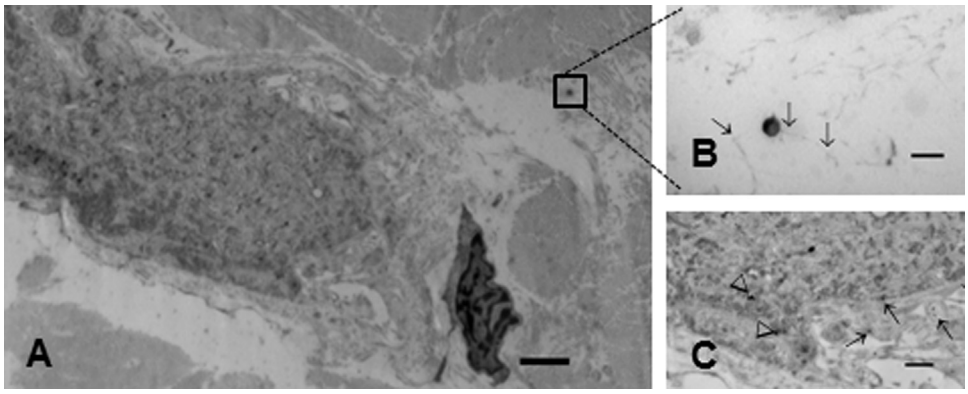

Fig. 7. A. Neuron in the muscularis mucosae. Scale bar: 2 μm. B. A higher power of the square in A shows the interstitial space around the neuron. A good example of an spherical combustion-derived nanoparticle (CDNP) with an attached fiber 11 nm in diameter (arrow). Scale bar: 100 nm. C. The neuronal nucleus with numerous euhedral NPs (arrowheads) and CDNPs (small arrow). Scale bar: 500 nm.

synuclein misfolding and aggregation" could indeed be NPs gaining access through the most vulnerable section of the GI tract: the small bowel (Johansson et al., 2013). The enteric nervous system is an ideal pathway to the brain (Visanji et al., 2014) and in keeping with the concept that the neuropathological process leading to PD starts in the ENS and/or the olfactory bulb and spread via rostrocraneal transmission via sympathetic and parasympathetic nervous system to the substantia nigrae and the CNS (Jellinger, 2014, 2015a, 2015b; Reichmann, 2011; Del Tredici and Braak, 2016) our current findings are pointing in the same direction.

There is no doubt that NPs play a role in protein aggregation and a superb example is the previously mentioned work of Alvarez and coworkers (Alvarez et al., 2013) showing gold NPs produce strong acceleration of α-synuclein aggregation and 10 nm particles produce the strongest effect. So, NPs traveling through axons (Gluska et al., 2016; Erriquez et al., 2015; Zhao et al., 2014; Kuznetsov, 2012; Osakada and

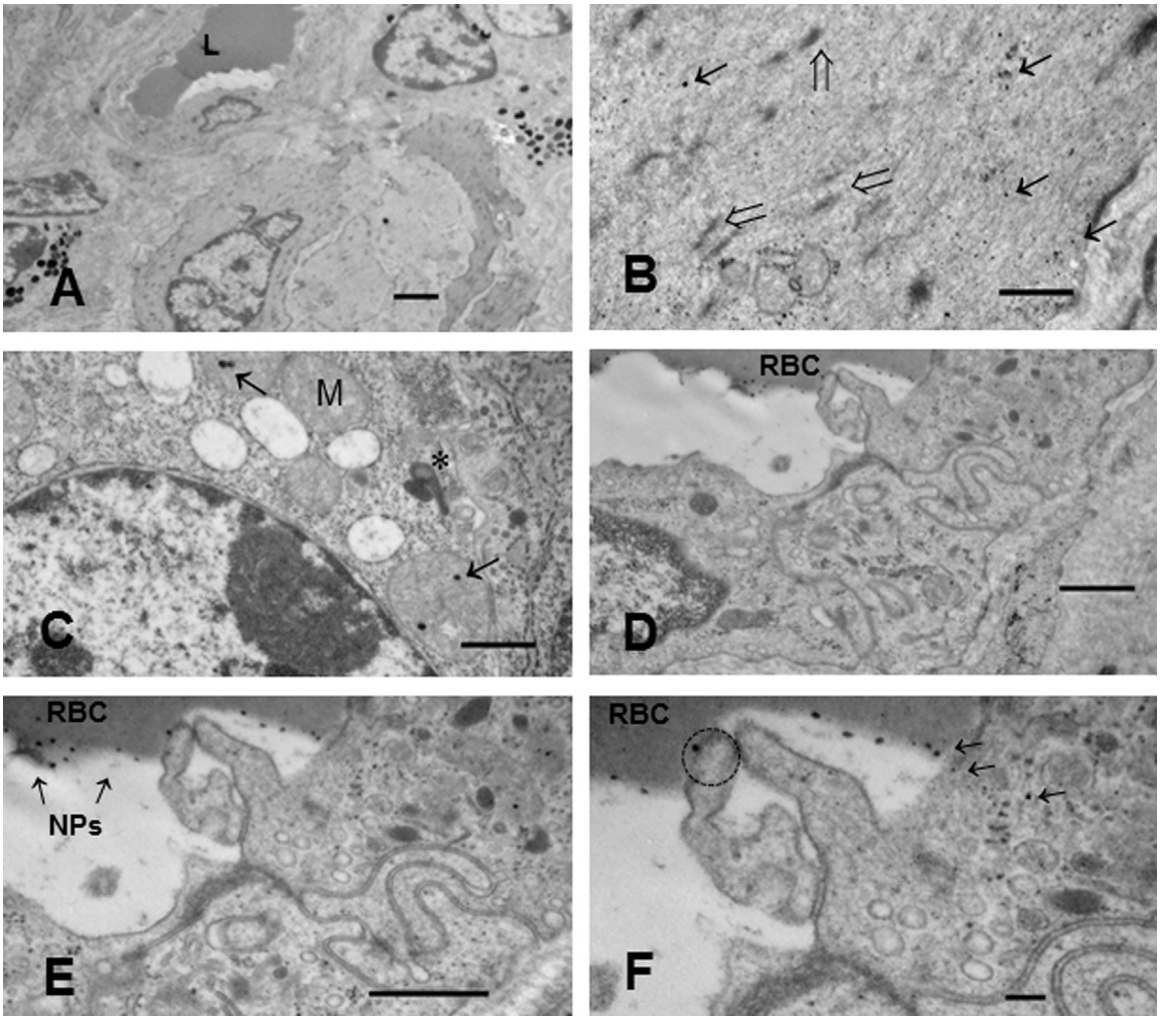

Fig. 8. A. Jejunal cryptal sample with blood vessels (L), smooth muscle cells and Paneth cells. Scale bar: 2 μm. B. The cytoplasm of a smooth muscle cell with numerous nanoparticles (short arrows), the dense bodies are marked with open head arrows. Scale bar: 500 nm. C. Lipofuscin structure is marked with * in this ganglion cell with numerous mitochondria (M) with NPs. Scale bar: 500 nm. D. F Two endothelial cells and a red blood cell (RBC) transferring nanoparticles to the endothelial cell. Notice the RBC with NPs in close contact with the endothelial cell and the passage of NPs in F (arrows). The caveolar activity is brisk in the endothelial cell. D, E Scale bar: 500 nm, F Scale bar: 100 nm.

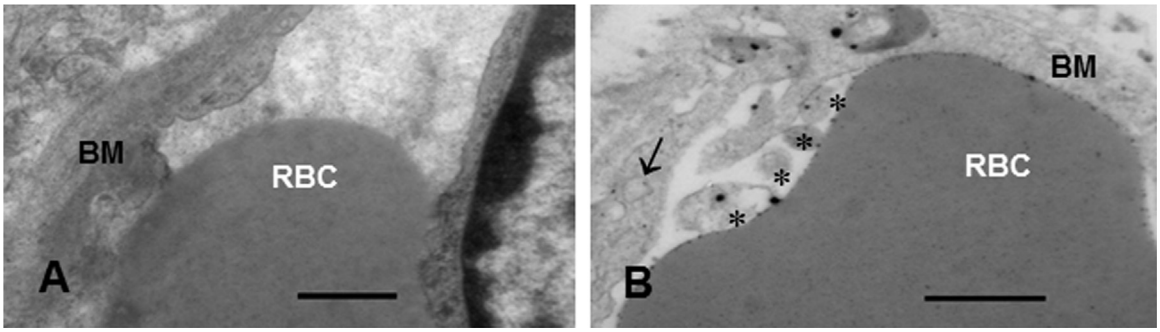

Fig. 9. An example of two capillaries in the submucosa of the duodenum, in A a control clean air animal and in B a Mexico City dog. A. The RBC is free of nanoparticles and the endothelial cell is not active. There is no ongoing caveolar formation. Scale bar: 500 nm. B. In contrast, the endothelial cell shows increased caveolar activity (arrow), fragments of the endothelial cell contain numerous nanoparticles (*) and NPs are already inside the endothelial cell cytoplasm. The arrow points to an irregular shape caveolar structure with one NP. Scale bar: 500 nm.

Cui, 2011; Hopkins et al., 2014; Vermehren-Schmaedick et al., 2014; Chowdary et al., 2015) could interfere with α-synuclein aggregation kinetics (Yu et al., 2009; Vácha et al., 2014; Mohammad-Beigi et al., 2015). On the same path, brain to stomach transfer of α-synuclein is not a surprise (Ulusoy et al., 2017) and provides further support the dorsal motor nucleus (DMN) of the vagus is a key relay center for α-synuclein transmission, and efferent vagal fibers may act as unique conduits for protein transfer. Indeed, the DMN is a key player in neuroinflammation in mice and children exposed to MC air pollution and shows a significant imbalance in genes for antioxidant defenses, apoptosis, and

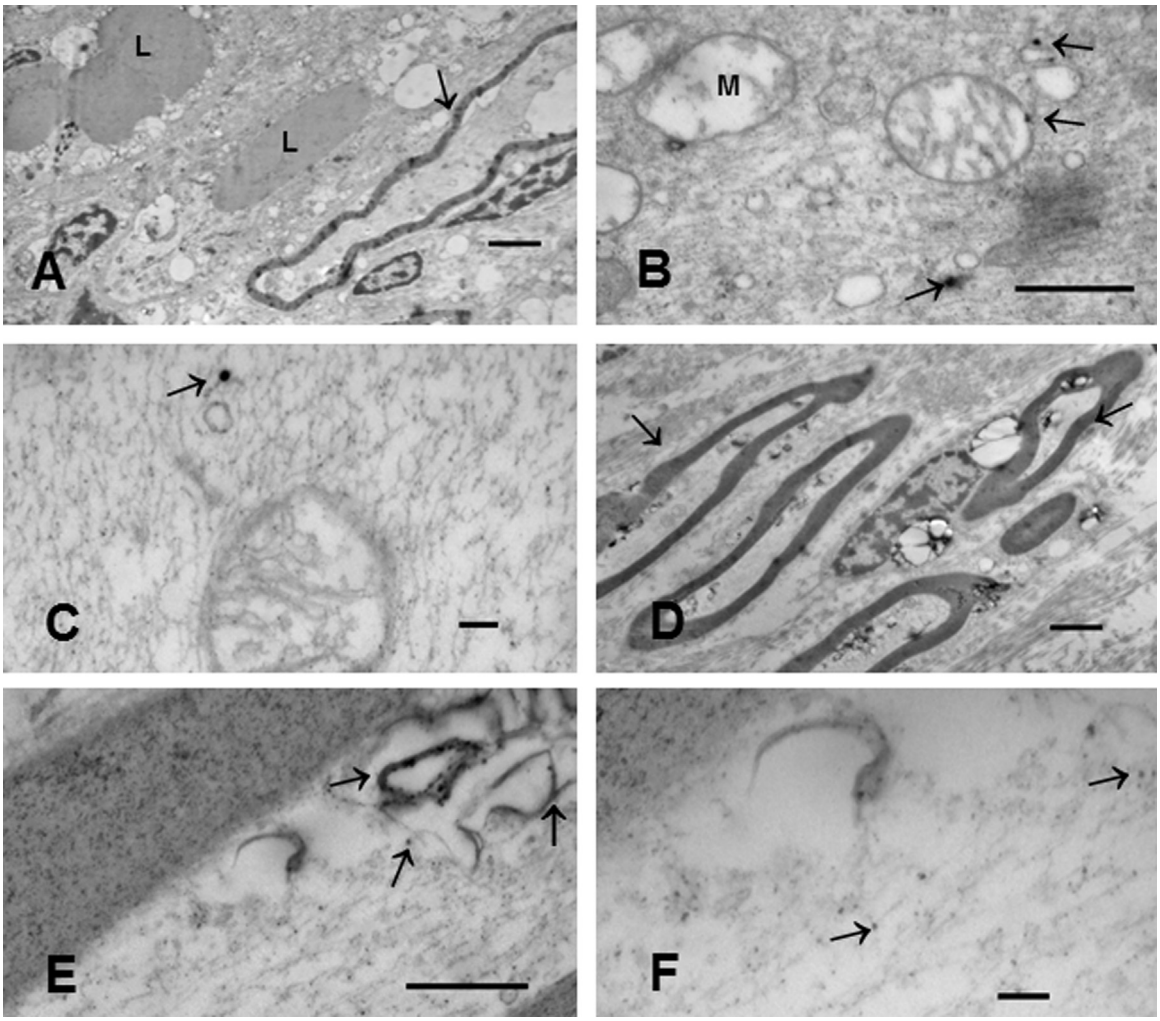

Fig. 10. Cervical vagal X electromicrographs. A–C Mexico City 17 year old male, 3/3 TLR4+, with +α-Syn and Htau in gastric samples, +α-Syn in vagus and negative vagal Htau (Supplementary Table 1). A Scale bar: 2 μm, B Scale bar: 500 nm, C Scale bar: 100 nm. A. Two blood vessels are seen and one large myelinated axon with an arrow. B. Axonal mitochondria (M) have abnormal cristae o no cristae and NPs are seen free in the axoplasm. C. Axonal abnormal mitochondria, a CDNP surrounded by microtubules and neurofilaments. D–F Mexico City 3 year old dog. D Scale bar: 100 nm, E Scale bar: 500 nm, F Scale bar: 100 nm. D. Significant damage to axons is shown here, the arrows point to focal fragmentation of myelin sheets. E. Lamellar, ill defined structures in the axoplasm. Notice the numerous clusters of NPs in the lamellar structures (arrows). F. NPs are numerous and free in the axoplasm (arrows).

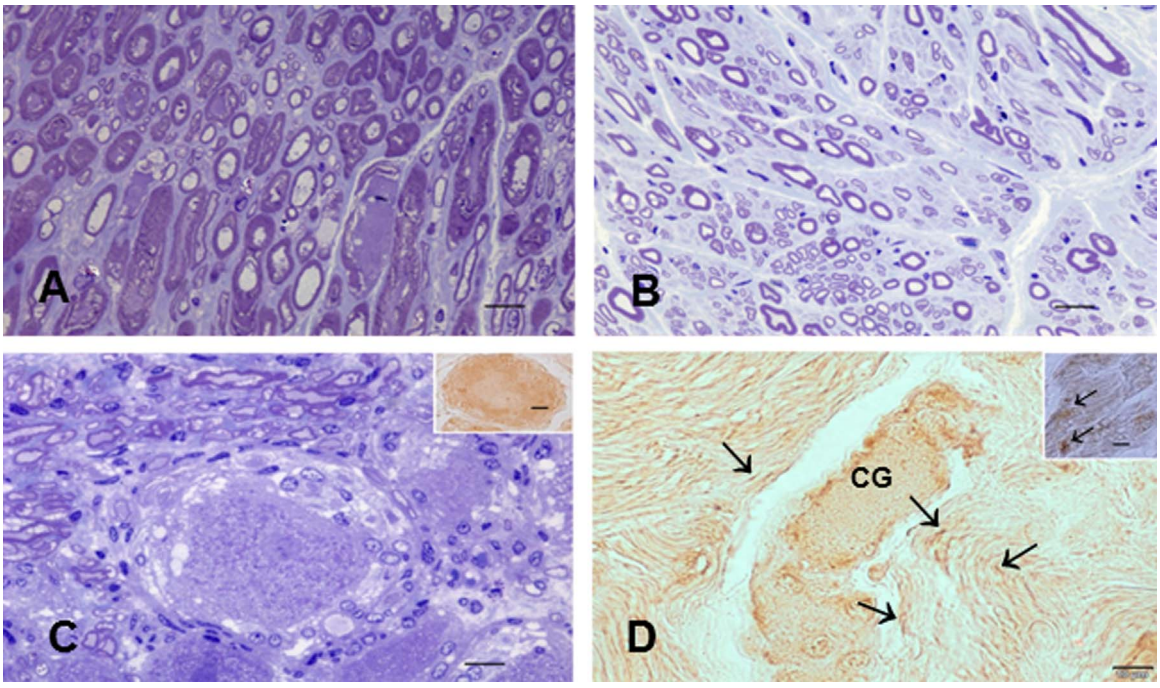

Fig. 11. Cervical vagus X samples. A. Mexico City 22 year old female toluidine blue 1 μm section of the vagus. A few isolated clusters of small myelinated axons.Scale bar: 10 μm. B. Mexico City 3 year old dog toluidine blue 1 μm section of the vagus. Perineural connective tissue is increased. Scale bar: 10 μm. C. Ganglion cells with a normal histological appearance contrast with the hyperphosphorylated aggregated α-synuclein (α-Syn) IR in the insert (product is brown with diaminobenzidine). Twenty year old MC male. Scale bar: 10 μm. D. Vagus nerve sections of a 3 year old male include a cluster of ganglion cells with a fine granular cytoplasmic IR α-Synand a few positive neurites (arrows). The + product is red with HIGHDEF ® Red IHC Chromogen. In the insert, aggregated α-synuclein (α-Syn) in neurites (arrows) with brown product in a 30 y old male. Scale bar: 10 μm. (For interpretation of the references to color in this figure legend, the reader is referred to the web version of this article.)

neurodegeneration (Villarreal-Calderon et al., 2010; Calderón-Garcidueñas et al., 2011).

Is the breakdown of the GI barrier and the involvement of the ENS key for the development of the early stages of Parkinson's disease we have already documented in Mexico City children? We strongly support a positive answer. The distribution of misfolded α synuclein in MC children and young adults follows precisely the early stages I and II of Braak's PD staging (Braak et al., 2003a, 2003b; Braak and Del Tredici, 2017). Exposed children have olfaction deficits and their olfactory bulbs show misfolded α-synuclein (Calderón-Garcidueñas et al., 2010).

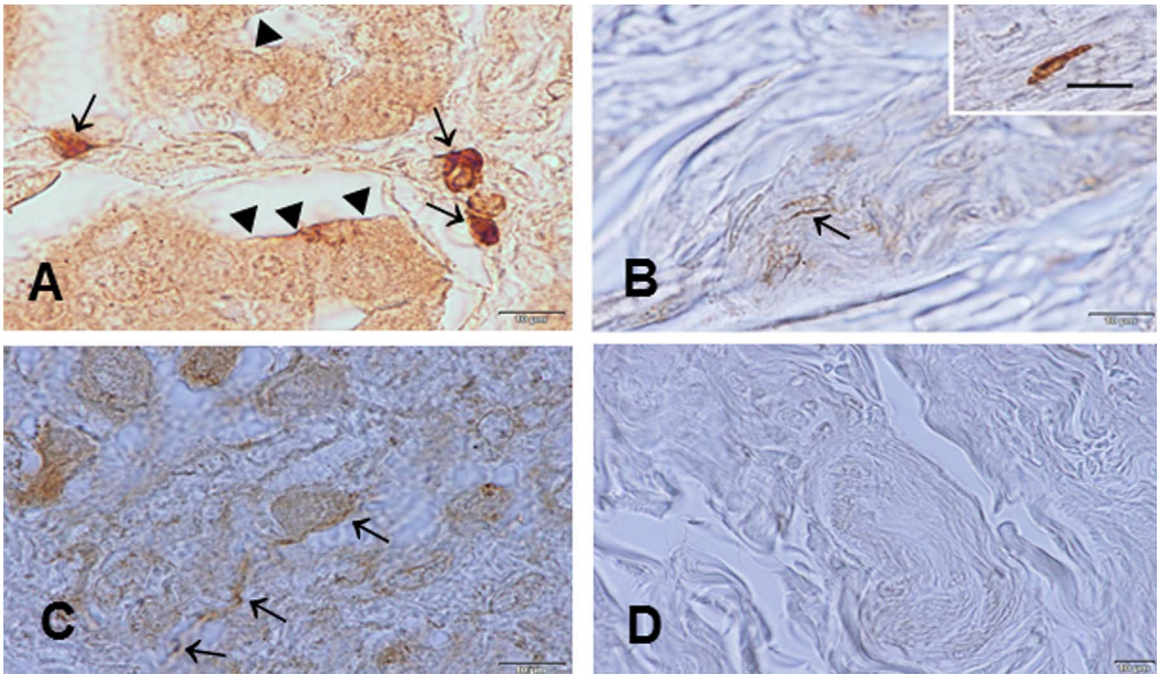

Fig. 12. Phosphorylated tau in gastric samples p-tau using mouse monoclonal antibody AT8 pSer202/Thr205 Scale bar: 10 μm. A. Eleven year old MC boy 3/3 TLR4+ with a few Htau+ nerve twigs throughout the gastric wall.This small bundle is in the submucosa, the insert shows a higher magnification of the + neurites. B. A MC 20 year old male, 3/3, TLR4+ shows IR Htau+ in axon terminals within neuromuscular junctions (*). C. A MC 30 year old male, 3/3, TLR4+ with IR Htau+ in submucosal and intramuscular nerves, coarse aggregates were present. D. A MC 34 year old male, 3/3, TLR4+ with IR Htau+ in ganglion cell clusters (arrows).

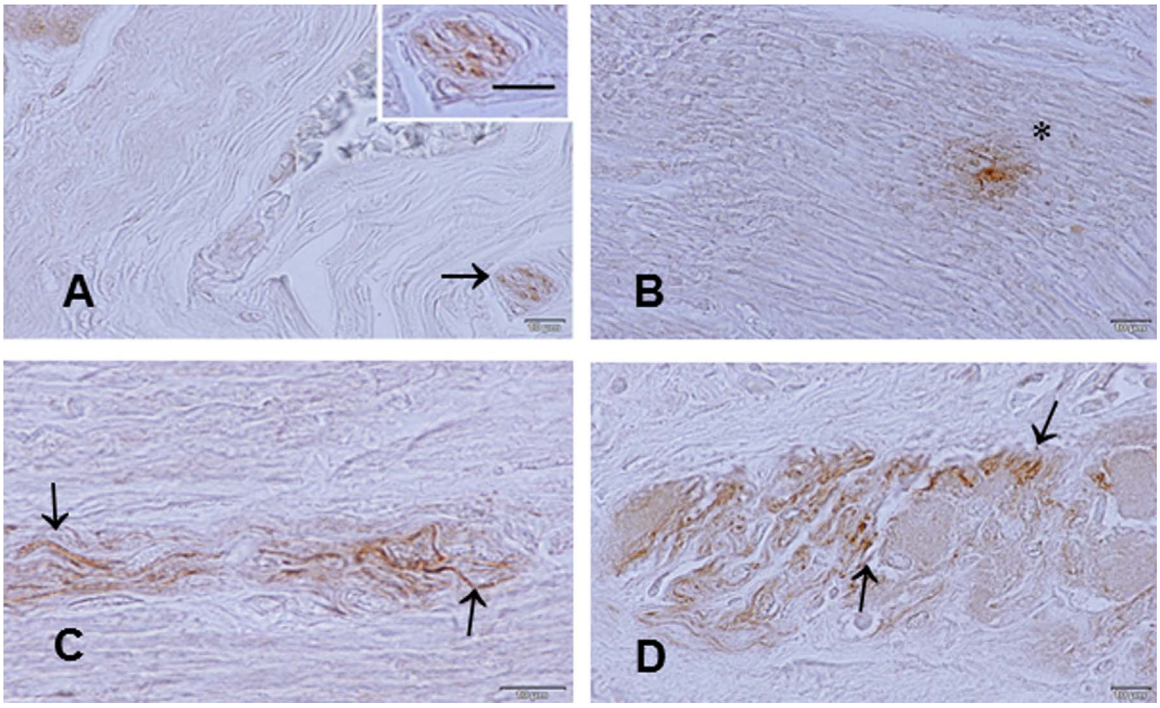

Fig. 13. Hyperphosphorylated aggregated α-synuclein (α-Syn) in gastric Mexico City children and teens. Scale bar: 10 μm. A. Gastric mucosa in a 3 year old male, 3/3, TLR4+, with negative Htau in gastric samples, +α-Syn in cervical X (Supplementary Table 1). Coarse +α-Syn (arrows) in S-100+ cells (not shown). Positive neurites are seen in glandular areas con arrow heads. B. Gastric sample from a 15 y male, 3/3, TLR 4+ numerous α-Syn immunoreactive intramuscular nerve twigs and axon terminals within neuromuscular junctions. Coarse α-Syn+ neurites were few (insert). C. Gastric sample from a MC 24 y old male 3/3, TLR 4+ with numerous α-Syn immunoreactive ganglion cells and long coarse + aggregates in neurites (arrows). D. A negative α-Syn immunoreactive 24 year old female control.

Olfactory dysfunction precedes the onset of motor symptoms by years (Doty, 2012), and the intranasal administration of neurotoxicants in experimental animals supports the olfactory vector hypothesis of Parkinson's disease (Prediger et al., 2012). The GI tract is a portal of entry of PM: 1. direct ingestion of inhaled PM is common after being mobilized up the trachea via the mucociliary escalator and the particle size determines if it is cleared out by cough or swallowing (Xi et al., 2012), 2. Children have large increases in ventilation and GI intake of particles with increasing activity (Stahlhofen et al., 1980; Lippmann et al., 1980; Brown et al., 2013), 3. PM enters in direct contact with the GI luminal components, the mucus layer and the microbiome (Johansson et al., 2013; Bergin and Witzmann, 2013), 4. NPs could gain direct access to the blood stream from the GI tract, while others damage the GI epithelial and endothelial barriers and alter the immune function (Kish et al., 2013; Johansson et al., 2013; Ermund et al., 2013; Douglas-Escobar et al., 2013; Bonazzi and Cossart, 2011; Klatt et al., 2010; Yang and Chiu, 2017). The GI anatomical compartments are differentially vulnerable to PM: According to Johansson and colleagues (Johansson et al., 2013), the small intestine would be the prime PM target: it has a single unattached mucus layer, NPs can have easy access to epithelial cells and to Peyer's patches, affecting immunosurveillance and altering epithelial integrity (Johansson et al., 2013; Mabbott et al., 2013; Lu et al., 2013). Of key importance to megacity residents is the fact the small intestinal barrier is immature in neonates, the anti-microbial peptide-dependent barrier function is weaker earlier in life (Birchenough et al., 2013) resulting in an exposure-threat present starting at the time of birth for urban dwelling residents. In fact, the youngest MC resident in this work is a 3 year old boy from a Northeast very polluted area in MC, he has hyperphosphorilated tau in frontal cortex and brainstem and has positive α-Syn in his olfactory bulbs. Moreover, this boy had a high 7.53 SIRM 77K in his frontal sample, capturing the magnetic contribution of ferromagnetic combustion-derived nanoparticles < 20 nm (Maher et al. (2016), Supplemental material). An obvious question in highly exposed populations particularly children is what happens to the turnover and neurogenesis of enteric neurons (Kulkarni et al., 2017), what is the extent of the damage in the dividing precursors needed to maintain enteric neuronal homeostasis (Veiga-Fernandes and Pachnis, 2017; Shea-Donohue and Urban, 2016)? If the enteric neuronal populations are compromised at an early age is this a risk factor for PD?

The American Gastroenterology Association and the American Psychosomatic Society share common interest in the key role of a functional intestinal microenvironment in brain-gut communication and -very relevant to Mexico City problems of violence-, the pathogenesis of neuropsychiatric and biopsychosocial disorders (Aroniadis et al., 2017). Mexico City has witnessed a steady increase in violent crime in the last decade along with a negative trust of authorities (Frías and Finkelhor, 2017; Ávila et al., 2016; Gómez-Dantés et al., 2016). Homicides, kidnappings, armed robberies, car thefts, and various forms of residential/street crime are every day concerns (Ávila et al., 2016), and none of the policies to decrease air pollution are working (Davis, 2017). It remains to be seen how high sustained exposures to air pollutants is impacting the pathogenesis of neuropsychiatric and biopsychosocial disorders in MC populations.

The severe damage to critical organelles in neurons, axons and dendrites has been discussed in the brain and the neuroenteric system in highly CDNP exposed individuals (Calderón-Garcidueñas et al., 2016a, 2010, 2011, 2013a, 2015a; González-Maciel et al., 2017), no surprises at all, since the extensive NPs literature has described their cellular toxicity (Gehr et al., 2011; Yu et al., 2013; Imam et al., 2015; Phukan et al., 2016; Harischandra et al., 2017). Thus, our novel finding of hyperphosphorylated tau in 66.6% of gastric samples in Mexico City young residents is in fact not a surprise either. These individuals have already extensive hyperphosphorylated tau in brainstem and frontal cortex and there is brain severe CDNPs associated pathology in mitochondria, endoplasmic reticulum, mitochondria-ER contacts, axons and dendrites (González-Maciel et al., 2017). The common denominator for the abnormal proteins are the high numbers and

concentrations of CDNPs in close contact with neurofilaments, microtubules, glial fibers, etc., altering microtubule dynamics, producing mitochondrial dysfunction, abnormal endosomal systems and resulting in accumulation and aggregation of unfolded proteins (González-Maciel et al., 2017). We can't ignore that seemingly healthy MC children already have significant cognitive deficits, affecting particularly overweight girls with an APOE 4 allele, young children with an APOE 4 share with their carrier parent low hippocampal NAA/Cr ratios or that they have significant food reward hormone dysregulation all related to their $PM_{2.5}$ exposures (Calderón-Garcidueñas et al., 2015a, 2015b, 2015c, 2015d, 2016a, 2016b, 2016c; Calderon-Garciduenas and de la Monte, 2017). Also in normal CSF samples, Aβ1-42 and BDNF concentrations are significantly lower in MC children versus controls ($p = 0.005$ and 0.02, respectively) (Calderón-Garcidueñas et al., 2016a). Our enteric nervous system (ENS) findings are in fact expected and biologically plausible.

The size of the nanoparticles in the ENS deserves a further comment. There is a significant difference in size between spherical exogenous CDNPs and the angular, and euhedral endogenous NPs in the brain versus the ENS.While in the brain the size of the CDNPs is on average 29.17 ± 11.22 nm and the endogenous euhedral NPs are 60.53 ± 14.6 nm, in the ENS the sizes are smaller 15.4 ± 6.0 and 21.2 ± 9.0 respectively. Moreover, the smallest CDNPs average size 11.85 ± 4.03 nm was measured in the cervical vagus, an interesting finding given that gold NPs 10 nm in diameter produced a 3-fold increase in the overall α-Syn aggregation rate at low concentrations in Alvarez et al., work. In sharp contrast, the largest CDNPs were found in the unmyelinated axons (21.99 ± 10.8 nm) which likely reflects a different access barrier and mode of transportation for CDNPs in small axons (see Fig. 5 and the increased subluminal caveolar activity of an endothelial cell in close proximity with an unmyelinated axon with CDNP). And since size does matter! The work of Alvarezet al. (Xie et al., 2016; Bermejo-Nogales et al., 2016) is highly relevant for exposed populations, because the damage to the ENS and the brain will depend on their sources of particulate matter and the sizes and composition of their nanoparticles and their magnetic capabilities. The issue of metal nanoparticles, magnetic hyperthermia, altered microtubule dynamics and signaling networks and cell changes in spatial self-organization have to be taken into account and the issue is complicated (Gheshlaghi et al., 2008; Min et al., 2013; Mao et al., 2015; Iannotti et al., 2017). For magnetic NPs with iron (such as the ones present in the brain of MC residents) the issues likely include interacting superparamagnetism and the oxidation of iron component as in Iannotti and coworkers paper (Iannotti et al., 2017). These type of NPs interactions are crucial for the nervous system cell components.

Where are we and where do we need to be? Looking forward and limitations

Cytotoxicity, membrane leakage, intracellular reactive oxygen species, misfolding of alpha-synuclein, mitochondrial dysfunction, strong acceleration of α-synuclein aggregation, inability of cells to regulate Ca^{2+}, neuroinflammation, and neurodegeneration are associated with the progressive damage of the nigrostriatal dopaminergic system and development of Parkinson's disease (PD) or a *syndrome* (?) (Titova et al., 2016). Combustion-derived nanoparticles are perfectly capable of producing dopaminergic cytotoxity through each one of the path mechanisms outlined above and certainly can travel through axons and dendrites (Levesque et al., 2011a, 2011b, 2013; Gehr et al., 2011; Alvarez et al., 2013; Harischandra et al., 2017; Phukan et al., 2016; Dönmez Güngüneş et al., 2017; Xie et al., 2016; Bermejo-Nogales et al., 2016; Gluska et al., 2016; Erriquez et al., 2015; Zhao et al., 2014; Kuznetsov, 2012; Osakada and Cui, 2011; Hopkins et al., 2014; Vermehren-Schmaedick et al., 2014; Chowdary et al., 2015; Vácha et al., 2014; Mohammad-Beigi et al., 2015). There is a complex interaction between neurofilaments (NFs) with other non-intermediate filament components of the cytoskeleton, including microtubules, and actin to establish a regionally specialized network that serves as a docking platform to organize other organelles and proteins (Yuan et al., 2017). We agreed with Titova and her group (Titova et al., 2016) that the *Parkinson's phenotype* is more a *dysfunctional multineurotransmitter pathway driven central and peripheral nervous system disorder*. We strongly argue that in the context of high air pollution exposures the neuropathology starts early in children and teens and contrary to current dogma [Prodromal PD delineated based upon age (Berg et al., 2015)], olfactory and brainstem involvement in childhood result in olfactory deficits and autonomic syntomatology. We certainly agree a 100% with Braak and Del Tredici (2017) that "*the earliest lesions* (in PD) *could develop at nonnigral (dopamine agonist nonresponsive) sites where the surrounding environment is potentially hostile: the olfactory bulb and, possibly, the ENS*".

While recognizing that the evaluations of the small bowel, vagus nerves and gastric samples were done in a small number of control and exposed subjects, the results are nonetheless important because they are not isolated and because they will help to guide future investigations covering the gaps between the NPs,the ENS and the development of Parkinson's disease in highly exposed young populations.

We fully agree with the current hypothesis that sporadic PD is a multiorgan relentless disease with genetic and environmental factors acting synergistically (Del Tredici and Braak, 2016), the data supporting axons of the nigrostriatal dopaminergic system are an early target of α-synuclein accumulation in PD (Caminiti et al., 2017), and we are strong supporters of the potential role of ubiquitous combustion-derived nanoparticles with high oxidative stress, cell toxicity and protein aggregation capabilities. NPs have anterograde, retrograde axonal and trans-synaptic trafficking capabilities and strong capacity for altering α-synuclein conformation and aggregation kinetics.

A key challenge is to characterize markers for the 'preclinical' and prodromal stages of the disease, identify populations at risk and define their neurotoxic air pollution exposures and in parallel measure CDNPs and markers of neuroinflammation in the brains and autonomic peripheral nervous system of young people with sudden accidental deaths. Early identification of children, teens and young adults at risk could enable the field to push into unchartered territory at the very beginning of the neuroinflammation and neurodegeneration process.

Highly oxidative, CDNPs constitute a novel path into Parkinson's pathogenesis.

5. Summary

Defining the linkage and the health consequences of the sustained prenatal and postnatal exposures to CDNPs upon brain/ gut/immune system interactions in children and young adults historically showing already the early hallmarks of Parkinson's disease ought to be of pressing importance for public health, may provide a fresh insight into Parkinson pathogenesis and open opportunities for early neuroprotection.

Acknowledgments

This work was partially supported by CONACYT Project 255956 G7 CB-2015-01.

Appendix A. Supplementary material

Supplementary data associated with this article can be found in the online version at http://dx.doi.org/10.1016/j.envres.2017.08.008.

References

Alvarez, Y.D., Fauerbach, J.A., Pellegrotti, J.V., Jovin, T.M., Jares-Erijman, E.A., Stefani, F.D., 2013. Influence of gold nanoparticles on the kinetics of α-synuclein aggregation. Nano Lett. 13, 6156–6163.

Aroniadis, O.C., Drossman, D.A., Simren, M.A., 2017. Perspective on brain-gut

communication: the American gastroenterology association and American psychosomatic society joint symposium on brain-gut interactions and the Intestinal microenvironment. Psychosom. Med. http://dx.doi.org/10.1097/PSY.0000000000000431.
Ávila, M.E., Martínez-Ferrer, B., Vera, A., Bahena, A., Musitu, G., 2016. Victimization, perception of insecurity, and changes in daily routines in Mexico. Rev. Saude Púb. 50 (0), 60.
Berg, D., Postuma, R.B., Adler, C.H., Bloem, B.R., Chan, P., Dubois, B., Gasser, T., Goetz, C.G., Halliday, G., Joseph, L., Lang, A.E., Liepelt-Scarfone, I., Litvan, I., Marek, K., Obeso, J., Oertel, W., Olanow, C.W., Poewe, W., Stern, M., Deuschl, G., 2015. MDS research criteria for prodromal Parkinson's disease. Mov. Disord. 30, 1600–1611.
Bergin, I.L., Witzmann, F.A., 2013. Nanoparticle toxicity by the gastrointestinal route: evidence and knowledge gaps. Int. J. Biomed. Nanosci. Nanotechnol. 3, 1–2.
Bermejo-Nogales, A., Fernandez, M., Fernandez-Cruz, M.L., Navas, J.M., 2016. Effects of a silver nanomaterial on cellular organelles and time course of oxidative stress in a fish cell line (PLHC-1). Comp. Biochem. Physiol. C Toxicol. Pharmacol. 190, 54–65.
Birchenough, G.M., Johansson, M.E., Stabler, R.A., Dalgakiran, F., Hansson, G.C., Wren, B.W., Luzio, J.P., Taylor, P.W., 2013. Altered innate defenses in the neonatal gastrointestinal tract in response to colonization by neuropathogenic Escherichia coli. Infect. Immun. 81, 3264–3275.
Braak, H., Rüb, U., Gai, W.P., Del Tredici, K., 2003a. Idiopathic Parkinson's disease: possible routes by which vulnerable neuronal types may be subject to neuroinvasion by an unknown pathogen. Neural Transm. 110, 517–536.
Braak, H., Del Tredici, K., Rüb, U., de Vos, R.A., Jansen Steur, E.N., Braak, E., 2003b. Staging of brain pathology related to sporadic Parkinson's disease. Neurobiol. Aging 24 (2), 197–211.
Braak, H., Del Tredici, K., 2017. Neuropathological staging of brain pathology in sporadic Parkinson's disease: separating the wheat from the chaff. J. Park. Dis. 7 (s1), S73–S87.
Bonazzi, M., Cossart, P., 2011. Impenetrable barriers or entry portals? The role of cell-cell adhesion during infection. J. Cell Biol. 195, 349–358.
Brown, J.S., Gordon, T., Price, O., Asgharian, B., 2013. Thoracic and respirable particle definitions for human health assessments. Part Fiber Toxicol. 10–12.
Calderón-Garcidueñas, L., Mora-Tiscareño, A., Fordham, L.A., Chung, C.J., García, R., Osnaya, N., Hernández, J., Acuña, H., Gambling, T.M., Villarreal-Calderón, A., Carson, J., Koren, H.S., Devlin, R.B., 2001. Canines as sentinel species for assessing chronic exposures to air pollutants: Part 1. Respiratory pathology. Toxicol. Sci. 61, 342–355.
Calderón-Garcidueñas, L., Solt, A.C., Henríquez-Roldán, C., Torres-Jardón, R., Nuse, B., Herritt, L., Villarreal-Calderón, R., Osnaya, N., Stone, I., García, R., Brooks, D.M., González-Maciel, A., Reynoso-Robles, R., Delgado-Chávez, R., Reed, W., 2008. Long-term air pollution exposure is associated with neuroinflammation, an altered innate immune response, disruption of the blood-brain-barrier, ultrafine particulate deposition, and accumulation of amyloid beta-42 and alpha-synuclein in children and young adults. Toxicol. Pathol. 36, 289–310.
Calderón-Garcidueñas, L., Macías-Parra, M., Hoffmann, H.J., Valencia-Salazar, G., Henríquez-Roldán, C., Osnaya, N., Monte, O.C., Barragán-Mejía, G., Villarreal-Calderón, R., Romero, L., Granada-Macías, M., Torres-Jardón, R., Medina-Cortina, H., Maronpot, R.R., 2009a. Immunotoxicity and environment: immunodysregulation and systemic inflammation in children. Toxicol. Pathol. 37, 161–169.
Calderón-Garcidueñas, L., Mora-Tiscareño, A., Gómez-Garza, G., Carrasco-Portugal, Mdel, C., Pérez-Guillé, B., Flores-Murrieta, F.J., Pérez-Guillé, G., Osnaya, N., Juárez-Olguín, H., Monroy, M.E., Monroy, S., González-Maciel, A., Reynoso-Robles, R., Villarreal-Calderon, R., Patel, S.A., Kumarathasan, P., Vincent, R., Henríquez-Roldán, C., Torres-Jardón, R., Maronpot, R.R., 2009b. Effects of a cyclooxygenase-2 preferential inhibitor in young healthy dogs exposed to air pollution: a pilot study. Toxicol. Pathol. 37 (5), 644–660.
Calderón-Garcidueñas, L., Franco-Lira, M., Henríquez-Roldán, C., González-Maciel, A., Reynoso-Robles, R., Villarreal-Calderon, R., Herritt, L., Brooks, B., Keefe, S., Palacios-Moreno, J., Villarreal-Calderon, R., Torres-Jardón, R., Medina-Cortina, H., Delgado-Chávez, R., Aiello-Mora, M., Maronpot, R.R., Doty, R.L., 2010. Olfactory dysfunction, olfactory bulb pathology and urban air pollution. Exp. Toxicol. Pathol. 62, 91–102.
Calderón-Garcidueñas, L., D'Angiulli, A., Kulesza, R.J., Torres-Jardón, R., Osnaya, N., Romero, L., Keefe, S., Herritt, L., Brooks, D.M., Avila-Ramirez, J., Delgado-Chávez, R., Medina-Cortina, H., González-González, L.O., 2011. Air pollution is associated with brainstem auditory nuclei pathology and delayed brainstem auditory evoked potentials. Int. J. Dev. Neurosci. 29, 365–375.
Calderón-Garcidueñas, L., Kavanaugh, M., Block, M.L., D'Angiulli, A., Delgado-Chávez, R., Torres-Jardón, R., González-Maciel, A., Reynoso-Robles, R., Osnaya, N., Villarreal-Calderón, R., Guo, R., Hua, Z., Zhu, H., Perry, G., Diaz, P., 2012. Neuroinflammation, hyperphosphorilated tau, diffuse amyloid plaques and down-regulation of the cellular prion protein in air pollution exposed children and adults. J. Alzheimers Dis. 28, 93–107.
Calderón-Garcidueñas, L., Franco-Lira, M., Mora-Tiscareño, A., Medina-Cortina, H., Torres-Jardón, R., Kavanaugh, M., 2013a. Early Alzheimer's and Parkinson's disease pathology in urban children: friend versus Foe responses-it is time to face the evidence. Biomed. Res. Int. 2013, 161687.
Calderón-Garcidueñas, L., Serrano-Sierra, A., Torres-Jardón, R., Zhu, H., Yuan, Y., Smith, D., Delgado-Chávez, R., Cross, J.V., Medina-Cortina, H., Kavanaugh, M., Guilarte, T.R., 2013b. The impact of environmental metals in young urbanites' brains. Exp. Toxicol. Pathol. 65, 503–511.
Calderón-Garcidueñas, L., Gónzalez-Maciel, A., Vojdani, A., Franco-Lira, M., Reynoso-Robles, R., Montesinos-Correa, H., Pérez-Guillé, B., Sarathi-Mukherjee, P., Torres-Jardón, R., Calderón-Garcidueñas, A., Perry, G., 2015a. The intestinal barrier in air pollution-associated neural involvement in Mexico City residents: mind the gut, the evolution of a changing paradigm relevant to Parkinson disease risk. J. Alzheimers Dis. Park. 5, 179.
Calderón-Garcidueñas, L., Mora-Tiscareño, A., Melo-Sánchez, G., Rodríguez-Díaz, J., Torres-Jardón, R., Styner, M., Mukherjee, P.S., Lin, W., Jewells, V., 2015b. A critical Proton MR Spectroscopy marker of Alzheimer's disease early neurodegenerative change: low hippocampal NAA/Cr ratio impacts APOE ε4 Mexico City children and their parents. J. Alzheimer Dis. 48, 1065–1075.
Calderón-Garcidueñas, L., Vojdani, A., Blaurock-Busch, E., Busch, I., Friedle, A., Franco-Lira, M., Sarathi-Mukherjee, P., Martínez-Aguirre, X., Park, S.B., Torres-Jardón, R., D'Angiulli, A., 2015c. Air pollution and children: neural and tight junction antibodies and combustion metals, the role of barrier breakdown and brain immunity in neurodegeneration. J. Alzheimers Dis. 43, 1039–1058.
Calderón-Garcidueñas, L., Franco-Lira, M., D'Angiulli, A., Rodríguez-Díaz, J., Blaurock-Busch, E., Busch, I., Chao, C.K., Thompson, C., Mukherjee, P.S., Torres-Jardón, R., Perry, G., 2015d. Mexico City normal weight children exposed to high concentrations of ambient PM2.5 show high blood leptin and endothelin-1, vitamin D deficiency and food reward hormone dysregulation versus low pollution controls. Relevance for obesity and Alzheimer disease. Environ. Res. 140, 579–592.
Calderón-Garcidueñas, L., Avila-Ramírez, J., Calderón-Garcidueñas, A., González-Heredia, T., Acuña-Ayala, H., Chao, C.K., Thompson, C., Ruiz-Ramos, R., Cortés-González, V., Martínez-Martínez, L., García-Pérez, M.A., Reis, J., Mukherjee, P.S., Torres-Jardón, R., Lachmann, I., 2016a. Cerebrospinal fluid biomarkers in highly exposed PM2.5 urbanites: the risk of Alzheimer's and Parkinson's diseases in Young Mexico City residents. J. Alzheimers Dis. 54, 597–613.
Calderón-Garcidueñas, L., Reynoso-Robles, R., Vargas-Martínez, J., Gómez-Maqueo-Chew, A., Pérez-Guillé, B., Sarathi-Mukherjee, P., Torres-Jardón, R., Perry, G., González-Maciel, A., 2016b. Prefrontal white matter pathology in air pollution exposed Mexico City young urbanites and their potential impact on neurovascular unit dysfunction and the development of Alzheimer's disease. Environ. Res. 146, 404–417.
Calderón-Garcidueñas, L., Jewells, V., Galaz-Montoya, C., van Zundert, B., Pérez-Calatayud, A., Ascencio-Ferrel, E., Valencia-Salazar, G., Sandoval-Cano, M., Carlos, E., Solorio, E., Acuña-Ayala, H., Torres-Jardón, R., D'Angiulli, A., 2016c. Interactive and additive influences of gender, BMI and Apolipoprotein 4 on cognition in children chronically exposed to high concentrations of PM2.5 and ozone.APOE4 females are at highest risk in Mexico City. Environ. Res. 150, 411–422.
Calderón-Garcidueñas, L., Villarreal-Ríos, R., 2017. Living close to heavy traffic roads, air pollution and dementia. Lancet 389, 675–677.
Calderón-Garcidueñas, L., de la Monte, S.M., 2017. Apolipoprotein E4, gender, body mass index, inflammation, insulin resistance and air pollution interactions: recipe for Alzheimer's disease development in Mexico City young females. J. Alzheimers Dis. 58, 613–630.
Caminiti, S.P., Presotto, L., Baroncini, D., Garibotto, V., Moresco, R.M., Gianolli, L., Volonté, M.A., Antonini, A., Perani, D., 2017. Axonal damage and loss of connectivity in nigrostriatal and mesolimbic dopamine pathways in early Parkinson's disease. Neuroimage Clin. 14, 734–740.
Chen, H., Kwong, J.C., Copes, R., Tu, K., Villeneuve, P.J., van Donkelaar, A., Hystad, P., Martin, R.V., Murray, B.J., Jessiman, B., Wilton, A.S., Kopp, A., Burnett, R.T., 2017. Living near major roads and the incidence of dementia, Parkinson's disease, and multiple sclerosis: a population-based cohort study. Lancet 389, 718–726.
Chow, A.K., Gulbransen, B.D., 2017. Potential roles of enteric glia in bridging neuroimmune communication in the gut. Am. J. Physiol. Gastrointest. Liver Physiol. 312, G145–G152.
Chowdary, P.D., Che, D.L., Kaplan, L., Chen, O., Pu, K., Bawendi, M., Cui, B., 2015. Nanoparticle-assisted optical tethering of endosomes reveals the cooperative function of dyneins in retrograde axonal transport. Sci. Rep. 5, 18059.
Corbillé, A.G., Preterre, C., Rolli-Derkinderen, M., Coron, E., Neunlist, M., Lebouvier, T., Derkinderen, P., 2017. Biochemical analysis of α-synuclein extracted from control and Parkinson's disease colonic biopsies. Neurosci. Lett. 641, 81–86.
Davis, L.W., 2017. Saturday driving restrictions fail to improve air quality in Mexico City. Sci. Rep. 7, 41652.
Del Tredici, K., Braak, H., 2016. Review: sporadic Parkinson's disease: development and distribution of α-synuclein pathology. Neuropathol. Appl. Neurobiol. 42, 33–50.
Dönmez Güngüneş, Ç., Şeker, Ş., Elçin, A.E., Elçin, Y.M., 2017. A comparative study on the in vitro cytotoxic responses of two mammalian cell types to fullerenes, carbon nanotubes and iron oxide nanoparticles. Drug Chem. Toxicol. 40, 215–227.
Douglas-Escobar, M., Elliot, E., Neu, J., 2013. Effect of intestinal microbial ecology on the developing brain. JAMA 167, 374–379.
Doty, R.L., 2012. Olfactory dysfunction in Parkinson disease. Nat. Rev. Neurol. 8, 329–339.
Ermund, A., Schütte, A., Johansson, M.E., Gustafsson, J.K., Hansson, G.C., 2013. Studies of mucus in mouse stomach, small intestine, and colon. I. Gastrointestinal mucus layers have different properties depending on location as well as over the Peyer's patches. Am. J. Physiol. Gastrointest. Liver Physiol. 305, G341–G347.
Erpapazoglou, Z., Mouton-Liger, F., Corti, O., 2017. From dysfunctional endoplasmic reticulum-mitochondria coupling to neurodegeneration. Neurochem. Int (pii, S0197-0186(17)30081-5).
Erriquez, J., Bolis, V., Morel, S., Fenoglio, I., Fubini, B., Quagliotto, P., Distasi, C., 2015. Nanosized TiO2 is internalized by dorsal root ganglion cells and causes damage via apoptosis. Nanomedicine 11, 1309–1319.
Fink, A.L., 2006. The aggregation and fibrillation of alpha-synuclein. Acc. Chem. Res. 39, 628–634.
Frías, S.M., Finkelhor, D., 2017. Victimizations of Mexican youth (12–17 years old): a 2014 national survey. Child Abus. Negl. 67, 86–97.
Gehr, P., Clift, M.J., Brandenberger, C., Lehmann, A., Herzog, F., Rothen-Rutishauser, B., 2011. Endocytosis of environmental and engineered micro-and nanosized particles. Comp. Physiol. 1, 1159–1174.
Gheshlaghi, Z.N., Riazi, G.H., Ahmadian, S., Ghafari, M., Mahinpour, R., 2008. Toxicity and interaction of titanium dioxide nanoparticles with microtubule protein. Acta Biochim. Biophys. Sin. 40, 777–782.

Giannoccaro, M.P., La Morgia, C., Rizzo, G., Carelli, V., 2017. Mitochondrial DNA and primary mitochondrial dysfunction in Parkinson's disease. Mov. Disord. 32, 346–363.
Gluska, S., Chein, M., Rotem, N., Ionescu, A., Perlson, E., 2016. Tracking Quantum-Dot labeled neurotropic factors transport along primary neuronal axons in compartmental microfluidic chambers. Methods Cell Biol. 131, 365–387.
Gómez-Dantés, H., Fullman, N., Lamadrid-Figueroa, H., Cahuana-Hurtado, L., Darney, B., Avila-Burgos, L., Correa-Rotter, R., Rivera, J.A., Barquera, S., González-Pier, E., Aburto-Soto, T., de Castro, E.F., Barrientos-Gutiérrez, T., Basto-Abreu, A.C., Batis, C., Borges, G., Campos-Nonato, I., Campuzano-Rincón, J.C., de Jesús Cantoral-Preciado, A., Contreras-Manzano, A.G., Cuevas-Nasu, L., de la Cruz-Gongora, V.V., Diaz-Ortega, J.L., de Lourdes García-García, M., Garcia-Guerra, A., de Cossío, T.G., González-Castell, L.D., Heredia-Pi, I., Hijar-Medina, M.C., Jauregui, A., Jimenez-Corona, A., Lopez-Olmedo, N., Magis-Rodríguez, C., Medina-Garcia, C., Medina-Mora, M.E., Mejia-Rodriguez, F., Montañez, J.C., Montero, P., Montoya, A., Moreno-Banda, G.L., Pedroza-Tobías, A., Pérez-Padilla, R., Quezada, A.D., Richardson-López-Collada, V.L., Riojas-Rodríguez, H., Ríos Blancas, M.J., Razo-Garcia, C., Mendoza, M.P., Sánchez-Pimienta, T.G., Sánchez-Romero, L.M., Schilmann, A., Servan-Mori, E., Shamah-Levy, T., Téllez-Rojo, M.M., Texcalac-Sangrador, J.L., Wang, H., Vos, T., Forouzanfar, M.H., Naghavi, M., Lopez, A.D., Murray, C.J., Lozano, R., 2016. Dissonant health transition in the states of Mexico, 1990–2013: a systematic analysis for the Global Burden of Disease Study 2013. Lancet 388, 2386–2402.
González-Maciel, A., Reynoso-Robles, R., Torres-Jardón, R., Mukherjee, P.S., Calderón-Garcidueñas, L., 2017. Combustion-derived nanoparticles in key brain target cells and organelles in young urbanites: culprit hidden in plain sight in Alzheimer's disease development. J. Alzheimers Dis. http://dx.doi.org/10.3233/JAD-170012.
Harischandra, D.S., Ghaisas, S., Rokad, D., Zamanian, M., Jin, H., Anantharam, V., Kimber, M., Kanthasamy, A., Kanthasamy, A., 2017. Environmental neurotoxicant manganese regulates exosome-mediated extracellular miRNAs in cell culture model of Parkinson's disease: relevance to α-synuclein misfolding in metal neurotoxicity. Neurotoxicology (pii, S0161-813X(17)30067-0).
Hawkes, C.H., Del Tredici, K., Braak, H., 2007. Parkinson's disease: a dual-hit hypothesis. Neuropathol. Appl. Neurobiol. 33, 599–614.
Hopkins, L.E., Patchin, E.S., Chiu, P.L., Brandenberger, C., Smiley-Jewell, S., Pinkerton, K.E., 2014. Nose-to-brain transport of aerosolised quantum dots following acute exposure. Nanotoxicology 8, 885–895.
Hu, X., Guo, F., Zhao, F., Fu, Z., 2017. Effects of titanium dioxide nanoparticles exposure on parkinsonism in zebra fish larvae and PC12. Chemosphere 173, 373–379.
Iannotti, V., Adamiano, A., Ausanio, G., Lanotte, L., Aquilanti, G., Coey, J.M.D., Lantieri, M., Spina, G., Fittipaldi, M., Margaris, G., Trohidou, K., Sprio, S., Montesi, M., Panseri, S., Sandri, M., Iafisco, M., Tampieri, A., 2017. Fe-doping-induced magnetism in nano-hydroxyapatites. Inorg. Chem. 56, 4447–4459.
Imam, S.Z., Lantz-McPeak, S.M., Cuevas, E., Rosas-Hernandez, H., Liachenko, S., Zhang, Y., Sarkar, S., Ramu, J., Robinson, B.L., Jones, Y., Gough, B., Paule, M.G., Ali, S.F., Binienda, Z.K., 2015. Iron oxide nanoparticles induce dopaminergic damage: in vitro pathways and in vivo imaging reveals mechanism of neuronal damage. Mol. Neurobiol. 52 (2), 913–926.
Jellinger, K.A., 2014. The pathomechanisms underlying Parkinson's disease. Expert Rev. Neurother. 14, 199–215.
Jellinger, K.A., 2015a. Neuropathobiology of non-motor symptoms in Parkinson disease. J. Neural Transm. 122, 1429–1440.
Jellinger, K.A., 2015b. How close are we to revealing the etiology of Parkinson's disease? Expert Rev. Neurother. 15, 1105–1107.
Johansson, M.E., Sjövall, H., Hansson, G.C., 2013. The gastrointestinal mucus system in health and disease. Nat. Rev. Gastroenterol. Hepatol. 10, 352–361.
Kirrane, E.F., Bowman, C., Davis, J.A., Hoppin, J.-A., Blair, A., Chen, H., Patel, M.M., Sandler, D.P., Tanner, C.M., Vinikoor-Imler, L., Ward, M.H., Luben, T.J., Kamel, F., 2015. Associations of ozone and PM2.5 concentrations with Parkinson's disease among participants in the agricultural health study. J. Occup. Environ. Med. 57, 509–517.
Kish, L., Hotte, N., Kaplan, G.G., Vincent, R., Tso, R., Gänzle, M., Rioux, K.P., Thiesen, A., Barkema, H.W., Wine, E., Madsen, K.L., 2013. Environmental particulate matter induces murine intestinal inflammatory responses and alters the gut microbiome. PLoS One 8 (4), e62220.
Klatt, N.R., Harris, L.D., Vinton, C.L., Sung, H., Briant, J.A., Tabb, B., Morcock, D., McGinty, J.W., Lifson, J.D., Lafont, B.A., Martin, M.A., Levine, A.D., Estes, J.D., Brenchley, J.M., 2010. Compromised gastrointestinal integrity in pigtail macaques is associated with increased microbial translocation, immune activation, and IL-17 production in the absence of SIV infection. Mucosal Immunol. 3, 387–398.
Kulkarni, S., Micci, M.A., Leser, J., Shin, C., Tang, S.C., Fu, Y.Y., Liu, L., Li, Q., Saha, M., Li, C., Enikolopov, G., Becker, L., Rakhilin, N., Anderson, M., Shen, X., Dong, X., Butte, M.J., Song, H., Southard-Smith, E.M., Kapur, R.P., Bogunovic, M., Pasricha, P.J., 2017. Adult enteric nervous system in health is maintained by a dynamic balance between neuronal apoptosis and neurogenesis. Proc. Natl. Acad. Sci. USA 114 (18), E3709–E3718.
Kuznetsov, A.V., 2012. Modelling transport of layered double hydroxide nanoparticles in axons and dendrites of cortical neurons. Comput. Methods Biomech. Biomed. Eng. 15 (12), 1263–1271.
Levesque, S., Surace, M.J., McDonald, J., Block, M.L., 2011a. Air pollution & the brain: subchronic diesel exhaust exposure causes neuroinflammation and elevates early markers of neurodegenerative disease. J. Neuroinflamm. 8, 105.
Levesque, S., Taetzsch, T., Lull, M.E., Kodavanti, U., Stadler, K., Wagner, A., Johnson, J.A., Duke, L., Kodavanti, P., Surace, M.J., Block, M.L., 2011b. Diesel exhaust activates and primes microglia: air pollution, neuroinflammation, and regulation of dopaminergic neurotoxicity. Environ. Health Perspect. 119, 1149–1155.
Levesque, S., Taetzsch, T., Lull, M.E., Johnson, J.A., McGraw, C., Block, M.L., 2013. The role of MAC1 in diesel exhaust particle-induced microglial activation and loss of dopaminergic neuron function. J. Neurochem. 125, 756–765.
Lindström, V., Gustafsson, G., Sanders, L.H., Howlett, E.H., Sigvardson, J., Kasrayan, A., Ingelsson, M., Bergström, J., Erlandsson, A., 2017. Extensive uptake of α-synuclein oligomers in astrocytes results in sustained intracellular deposits and mitochondrial damage. Mol. Cell Neurosci (pii: S1044-7431)(16)(30184-1).
Lippmann, M., Yeates, D.B., Albert, R.E., 1980. Deposition, retention and clearance of inhaled particles. Br. J. Ind. Med. 37, 337–362.
Liu, R., Young, M.T., Chen, J.C., Kaufman, J.D., Chen, H., 2016. Ambient air pollution exposures and risk of Parkinson disease. Environ. Health Perspect. 124, 1759–1765.
Liu, S.Y., Chan, P., Stoessl, A.J., 2017. The underlying mechanism of prodromal PD: insights from the parasympathetic nervous system and the olfactory system. Transl. Neurodegener. 6, 4.
Lu, Z., Ding, L., Lu, Q., Chen, Y.H., 2013. Claudins in intestines: distribution and functional significance in health and diseases. Tissue Barriers 1, e24978.
Mabbott, N.A., Donaldson, D.S., Ohno, H., Williams, I.R., Mahajan, A., 2013. Microfold (M) cells: important immunosurveillance posts in the intestinal epithelium. Mucosal Immunol. 6, 666–677.
Maher, B.A., Ahmed, I.A., Karloukovski, V., MacLaren, D.A., Foulds, P.G., Allsop, D., Mann, D.M., Torres-Jardón, R., Calderon-Garciduenas, L., 2016. Magnetite pollution nanoparticles in the human brain. Proc. Natl. Acad. Sci. USA 113 (39), 10797–10801.
Mao, Z., Xu, B., Ji, X., Zhou, K., Zhang, X., Chen, M., Han, X., Tang, Q., Wang, X., Xia, Y., 2015. Titanium dioxide nanoparticles alter cellular morphology via disturbing the microtubule dynamics. Nanoscale 7, 8466–8475.
Massano, J., Bhatia, K.P., 2012. Clinical approach to Parkinson's disease: features, diagnosis, and principles of management. Cold Spring Harb. Perspect. Med. 2 (6), a008870.
McMenamin, C.A., Travagli, R.A., Browning, K.N., 2016. Inhibitory neurotransmission regulates vagal efferent activity and gastric motility. Exp. Biol. Med. 241 (12), 1343–1350.
Min, K.A., Shin, M.C., Yu, F., Yang, M., David, A.E., Yang, V.C., Rosania, G.R., 2013. Pulsed magnetic field improves the transport of iron oxide nanoparticles through cell barriers. ACS Nano 7, 2161–2171.
Mohammad-Beigi, H., Shojaosadati, S.A., Marvian, A.T., Pedersen, J.N., Klausen, L.H., Christiansen, G., Pedersen, J.S., Dong, M., Morshedi, D., Otzen, D.E., 2015. Strong interactions with polyethylenimine-coated human serum albumin nanoparticles (PEI-HSA NPs) alter α-synuclein conformation and aggregation kinetics. Nanoscale 7, 19627–19640.
Molina, L.T., Madronich, S.J., Gaffney, J.S., Apel, E., de Foy, B., Fast, J., Ferrare, R., Herndon, S., Jimenez, J.L., Lamb, B., Osornio-Vargas, A.R., Russell, P., Schauer, J.J.P., Stevens, S., Volkamer, E., Zavala, M., 2010. An overview of the MILAGRO. (2006). Campaign: Mexico City emissions and their transport and transformation. Atmos. Chem. Phys. 10, 8697–8760.
Okita, Y., Rcom-H'cheo-Gauthier, A.N., Goulding, M., Chung, R.S., Faller, P., Pountney, D.L., 2017. Metallothionein, copper and alpha-synuclein in alpha-synucleinopathies. Front. Neurosci. 11, 114.
Osakada, Y., Cui, B., 2011. Real-time visualization of axonal transport in neurons. Methods Mol. Biol. 670, 231–243.
Phukan, G., Shin, T.H., Shim, J.S., Paik, M.J., Lee, J.K., Choi, S., Kim, Y.M., Kang, S.H., Kim, H.S., Kang, Y., Lee, S.H., Mouradian, M.M., Lee, G., 2016. Silica-coated magnetic nanoparticles impair proteasome activity and increase the formation of cytoplasmic inclusion bodies in vitro. Sci. Rep. 6, 29095.
Powley, T.L., Hudson, C.N., McAdams, J.L., Baronowsky, E.A., Phillips, R.J., 2016. Vagal intramuscular arrays: the specialized mechanoreceptor arbors that innervate the smooth muscle layers of the stomach examined in the rat. J. Comp. Neurol. 524, 713–737.
Prediger, R.D., Aquiar Jr., A.S., Matheus, F.C., Walz, R., Antoury, L., Raisman-Vozari, R., Doty, R.L., 2012. Intranasal administration of neurotoxicants in animals: support for the olfactory vector hypothesis of Parkinson's disease. Neurotox. Res. 21, 90–116.
Querol, X., Pey, J., Minguillón, M.C., Pérez, N., Alastuey, A., Viana, M., Moreno, T., Bernabé, R.M., Blanco, S., Cárdenas, B., Vega, E., Sosa, G., Escalona, S., Ruiz, H., Artíñano, B., 2008. PM speciation and sources in Mexico during the MILAGRO-2006 Campaign. Atmos. Chem. Phys. 8, 111–128.
Reichmann, H., 2011. Viewpoint: etiology in Parkinson's disease. Dual hit or spreading intoxication. J. Neurol. Sci. 310 (1–2), 9–11.
Rocha, E.M., De Miranda, B., Sanders, L.H., 2017. Alpha-synuclein: pathology, mitochondrial dysfunction and neuroinflammation in Parkinson's disease. Neurobiol. Dis (pii: S0969-9961)(17)(30080-3).
Rodriguez, J.A., Ivanova, M.I., Sawaya, M.R., Cascio, D., Reyes, F.E., Shi, D., Sangwan, S., Guenther, E.L., Johnson, L.M., Zhang, M., Jiang, L., Arbing, M.A., Nannenga, B.L., Hattne, J., Whitelegge, J., Brewster, A.S., Messerschmidt, M., Boutet, S., Sauter, N.K., Gonen, T., Eisenberg, D.S., 2015. Structure of the toxic core of α-synuclein from invisible crystals. Nature 525 (7570), 486–490.
Rosas Pérez, I., Serrano, J., Alfaro-Moreno, E., Baumgardner, D., García-Cuellar, C., Martín Del Campo, J.M., Raga, G.B., Castillejos, M., Colín, R.D., Osornio Vargas, A.R., 2007. Relations between PM_{10} composition and cell toxicity: a multivariate and graphical approach. Chemosphere 67, 1218–1228.
Santurtún, A., Delgado-Alvarado, M., Villar, A., Riancho, J., 2016. Geographical distribution of mortality by Parkinson's disease and its association with air lead levels in Spain. Med. Clin. 147, 481–487.
Scott, L., Dawson, V.,L., Dawson, T.M., 2017. Trumping neurodegeneration: targeting common pathways regulated by autosomal recessive Parkinson's disease genes. Exp. Neurol (pii, S0014-4886(17)30102-4).
Secretaría del Medio Ambiente Gobierno del Distrito Federal (SMA-GDF), 2012. Inventario de Emisiones Zona Metropolitana del Valle de México. Contaminantes Criterio 2010. 〈http://www.sma.df.gob.mx/sma/links/download/biblioteca/inventarios_emisiones2010/IEcriterio10_.pdf〉.

Shea-Donohue, T., Urban Jr., J.F., 2016. Neuroimmune modulation of gut function. Handb. Exp. Pharmacol. http://dx.doi.org/10.1007/164_2016_109.

Stahlhofen, W., Gebhart, J., Heyder, J., 1980. Experimental determination of the regional deposition of aerosol particles in the human respiratory tract. Am. Ind. Hyg. Assoc. J. 41, 385–398.

Ting, S.J., Kao, C.K., Wang, F.B., 2017. Double labeling of vagal preganglionic and sympathetic postganglionic fibers in celiac ganglion, superior mesenteric arteries and myenteric plexus. Chin. J. Physiol. 60 (1), 41–53.

Titova, N., Padmakumar, C., Lewis, S.J., Chaudhuri, K.R., 2016. Parkinson's: a syndrome rather than a disease? J. Neural Transm. http://dx.doi.org/10.1007/s00702-016-1667-6.

Uesaka, T., Young, H.M., Pachnis, V., Enomoto, H., 2016. Development of the intrinsic and extrinsic innervation of the gut. Dev. Biol. 417 (2), 158–167.

Ulusoy, A., Phillips, R.J., Helwig, M., Klinkenberg, M., Powley, T.L., Di Monte, D.A., 2017. Brain-to-stomach transfer of α-synuclein via vagal preganglionic projections. Acta Neuropathol. 133 (3), 381–393.

Vácha, R., Linse, S., Lund, M., 2014. Surface effects on aggregation kinetics of amyloidogenic peptides. J. Am. Chem. Soc. 136 (33), 11776–11782.

Vega, E., Ruiz, H., Escalona, S., Cervantes, A., Lopez–Veneroni, D., Gonzalez–Avalos, E., Sanchez–Reyna, G., 2011. Chemical composition of fine particles in Mexico City during 2003–2004. Atmos. Pollut. Res. 2, 477–483.

Veiga-Fernandes, H., Pachnis, V., 2017. Neuroimmune regulation during intestinal development and homeostasis. Nat. Immunol. 18, 116–122.

Vermehren-Schmaedick, A., Krueger, W., Jacob, T., Ramunno-Johnson, D., Balkowiec, A., Lidke, K.A., Vu, T.Q., 2014. Heterogeneous intracellular trafficking dynamics of brain-derived neurotrophic factor complexes in the neuronal soma revealed by single quantum dot tracking. PLoS One 9, e95113.

Villarreal-Calderon, R., Torres-Jardón, R., Palacios-Moreno, J., Osnaya, N., Pérez-Guille, B., Maronpot, R.R., Reed, W., Zhu, H., Calderón-Garcidueñas, L., 2010. Urban air pollution targets the dorsal vagal complex and dark chocolate offers neuroprotection. Int. J. Toxicol. 29, 604–615.

Visanji, N.P., Marras, C., Hazrati, L.N., Liu, L.W.C., Lang, A.E., 2014. Alimentary, my dear Watson? The challenges of enteric α-synuclein as a Parkinson's disease biomarker. Mov. Disord. 29, 444–450.

Volk, N., Lacy, B., 2017. Anatomy and physiology of the small bowel. Gastrointest. Endosc. Clin. N. Am. 27 (1), 1–13.

Vuong, H.E., Yano, J.M., Fung, T.C., Hsiao, E.Y., 2017. The microbiome and host behavior. Annu. Rev. Neurosci. http://dx.doi.org/10.1146/annurev-neuro-072116-031347. (Epub ahead of print).

Walter, G.C., Phillips, R.J., McAdams, J.L., Powley, T.L., 2016. Individual sympathetic postganglionic neurons coinnervate myenteric ganglia and smooth muscle layers in the gastrointestinal tract of the rat. J. Comp. Neurol. 524, 2577–2603.

Wang, Y., Liu, D., Zhang, H., Wang, Y., Wei, L., Liu, Y., Liao, J., Gao, H.M., Zhou, H., 2017. Ultrafine carbon particles promote rotenone-induced dopamine neuronal loss through activating microglial NADPH oxidase. Toxicol. Appl. Pharmacol. 322, 51–59.

Xi, J., Berlinski, A., Zhou, Y., Greenberg, B., Ou, X., 2012. Breathing resistance and ultrafine particle deposition in nasal-laryngeal airways of a newborn, an infant, a child, and an adult. J. Biomed. Eng. 40, 2579–2595.

Xie, H., Wu, J., 2016. Silica nanoparticles induce alpha-synuclein induction and aggregation in PC12-cells. Chem. Biol. Interact. 258, 197–204.

Xie, Y., Liu, D., Cai, C., Chen, X., Zhou, Y., Wu, L., Sun, Y., Dai, H., Kong, X., Liu, P., 2016. Size-dependent cytotoxicity of Fe3O4 nanoparticles induced by biphasic regulation of oxidative stress in different human hepatoma cells. Int. J. Nanomed. 11, 3557–3570.

Yang, N.J., Chiu, I.M., 2017. Bacterial signaling to the nervous system through toxins and metabolites. J. Mol. Biol. 429 (5), 587–605.

Yu, J., Lyubchenko, Y.L., 2009. Early stages for Parkinson's development: alpha-synuclein misfolding and aggregation. J. Neuroimmune Pharmacol. 4 (1), 10–16.

Yu, S.H., Tang, D.W., Hsieh, H.Y., Wu, W.S., Lin, B.X., Chuang, E.Y., Sung, H.W., Mi, F.L., 2013. Nanoparticle-induced tight-junction opening for the transport of an anti-angiogenic sulfated polysaccharide across Caco-2 cell monolayers. Acta Biomater. 9, 7449–7459.

Yuan, A., Rao, M.V., Veeranna, Nixon, R.A., 2017. Neurofilaments and neurofilament proteins in health and disease. Cold Spring Harb. Perspect. Biol. 9 (4), a018309.

Zaichick, S.V., McGrath, K.M., Caraveo, G., 2017. The role of Ca2+ signaling in Parkinson's disease. Dis. Model Mech. 10 (5), 519–535.

Zhao, X., Zhou, Y., Weissmiller, A.M., Pearn, M.L., Mobley, W.C., Wu, C., 2014. Real-time imaging of axonal transport of quantum dot-labeled BDNF in primary neurons. J. Vis. Exp. 91, 51899.